EGG-TMI-7429
July 1987

INFORMAL REPORT

TMI-2 LOWER PLENUM VIDEO DATA SUMMARY

James P. Adams
Richard P. Smith

Idaho National Engineering Laboratory

Managed by the U.S. Department of Energy

EG&G Idaho

Work performed under DOE Contract No. DE-AC07-76ID01570

EGG-TMI-7429

TMI-2 LOWER PLENUM VIDEO DATA SUMMARY

James P. Adams
Richard P. Smith

Published July 1987

EG&G Idaho, Inc.
Idaho Falls, Idaho 83415

Prepared for the
U.S. Department of Energy
Idaho Operations Office
Under DOE Contract No. DE-AC07-76ID01570

ABSTRACT

The best-estimate configuration of the TMI-2 lower plenum debris bed is displayed based on an analysis of video data. The data were taken using remotely controlled video cameras inserted in the downcomer in February, July, and December 1985, as well as during core bore operations in July 1986. The visual composition and extent of the debris bed are characterized, and the mass of core material which relocated to the lower plenum during the accident is estimated.

SUMMARY

Remotely controlled video cameras were inserted into access holes at various azimuthal locations in the TMI-2 downcomer in February, July, and December 1985. These cameras were lowered into the lower plenum and were used to record video data of the core material which had relocated from the core region during the March 1979 accident, forming a debris bed in the lower plenum. Additional video data of the lower plenum debris bed were recorded during core boring operations in July 1986.

These video data were analyzed, and the lower plenum debris bed has been characterized. Large inhomogeneities exist in the physical appearance of the debris bed, ranging from a very fine, dust-like and smooth surface, to a relatively flat but coarse surface with large chunks, to an apparently solid "wall" of lava-like debris.

A topography was derived from a series of measurements of the debris bed depth, and this topography was used to provide an estimate for the debris bed volume of 4.85 ± 1.21 m^3. This volume was combined with estimates of the mass density of 7.0 g/cm^3 (obtained from grab samples) and porosity of 0.45 to derive the estimated total mass of corium which relocated to the lower plenum during the accident, 15 ± 5 metric tons.

ACKNOWLEDGMENTS

The authors would like to express their thanks to the following for their assistance in preparing this report: W. F. Downs, E. L. Tolman, M. L. Russell, S. Langer, D. J. Osetek, and J. M. Broughton, for helpful discussion and draft review; D. E. Owen, G. R. Eidam, and G. Worku, for assistance in obtaining the data; and N. L. Wade, for exceptional editorial support and patience.

CONTENTS

FIGURES

TABLES

TMI-2 LOWER PLENUM VIDEO DATA SUMMARY

INTRODUCTION

Since the accident at the Three Mile Island Unit 2 (TMI-2) nuclear power plant in March 1979, a great deal of effort has been expended in understanding the accident. These efforts have included detailed examination of the thermal and hydraulic data recorded during the accident; examination of samples removed from the core, upper plenum, reactor building, etc.; and in-depth calculations of the accident progression. This report summarizes information gleaned from an additional data source: visual data taken using remote cameras inserted into the lower plenum of the reactor vessel.

A total of five visual examinations have been made of parts of the lower plenum. The first examination occurred in February 1985[1,2] when a camera was sequentially inserted into two different access holes in the downcomer. These holes are labeled 4 and 11 on Figure 1, which is a schematic of the reactor vessel cross section and illustrates those areas of the lower plenum which have been visually examined. This first examination included those areas of the lower plenum around the Z and X axes.

The second examination took place in July 1985;[3] a camera was inserted into holes 7 and 8 (near the W axis), hole 1 (near the Y axis) and hole 11 (near the X axis). During this inspection, a remote sampler was used to extract samples of the rubble near the W and X axes. The results of the examination of these samples are reported in Reference 4. Subsequent to the sampling, a water jet, with an attached camera, was inserted into hole 11 and an attempt was made to move the debris using high-pressure water.[5] The water jet was able to move the finely divided debris, indicating that the debris bed was fairly loose, rather than a solid mass.

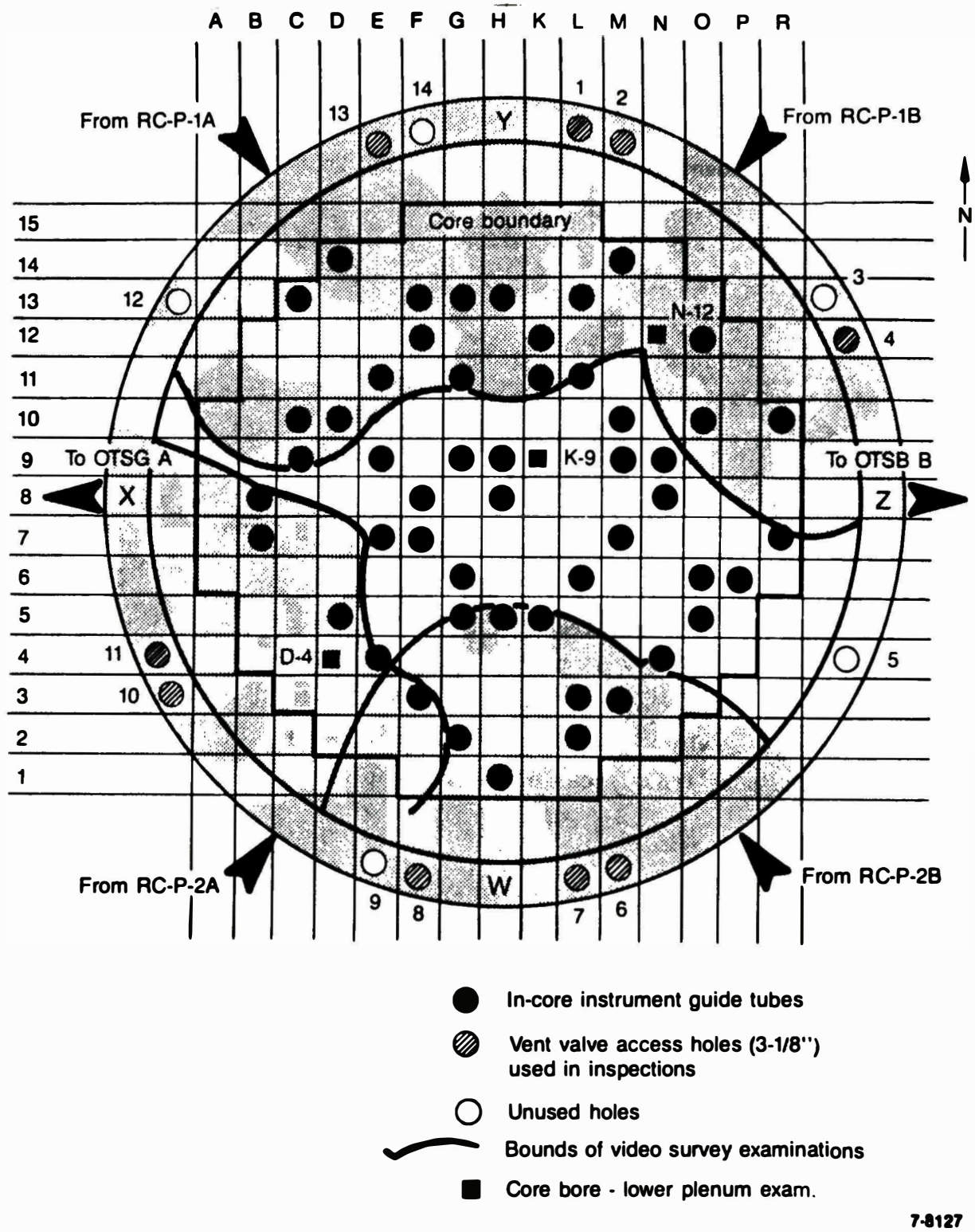

Figure 1. TMI-2 core map, illustrating the extent of video data.

The third visual examination occurred in December 1985,[6] when the areas near the Y axis (via hole 14), W axis (hole 7), and X-axis (hole 11) were examined. During this visual examination period, a remote manipulator was also inserted through an adjacent hole. The manipulator was used to position the camera so that a wider area could be examined. This included routing the camera up through several flow holes in the elliptical flow distributor head to examine the core support assembly (CSA) region between the elliptical flow distributor and the instrument support plate. This region is illustrated in Figure 2.

The core stratification sampling program (core bore) was conducted in July 1986.[7] As part of this program, a camera was inserted into holes bored through the consolidated part of the core and lowered as far as possible to examine the lower CSA. In three cases, corresponding to fuel assembly locations D-4, K-9, and N-12, the holes extended into the lower plenum region and the rubble bed could be examined. These three locations are also indicated on Figure 1.

Following acquisition of the core bore samples, the boring equipment was used to drill more than 400 11.4-cm-diam holes in the core crust in an effort to break up the core for defueling.[8] During this operation, approximately 4.2 metric tons of additional core debris sifted into the lower plenum and settled onto the existing debris bed.[9]

The last lower plenum video inspection was conducted in February, 1987, subsequent to the core drilling operation.[10] Since the topography of the debris bed had been significantly altered by the additional debris from the boring operation, no additional information was gained regarding the postaccident depth or configuration. However, a damaged in-core instrument guide tube was examined.

This report summarizes the video data which were taken during these five lower plenum examinations. First, the topography of the lower plenum rubble bed is discussed; and then the physical appearance of the rubble bed is treated. Appendix A presents a detailed description of the

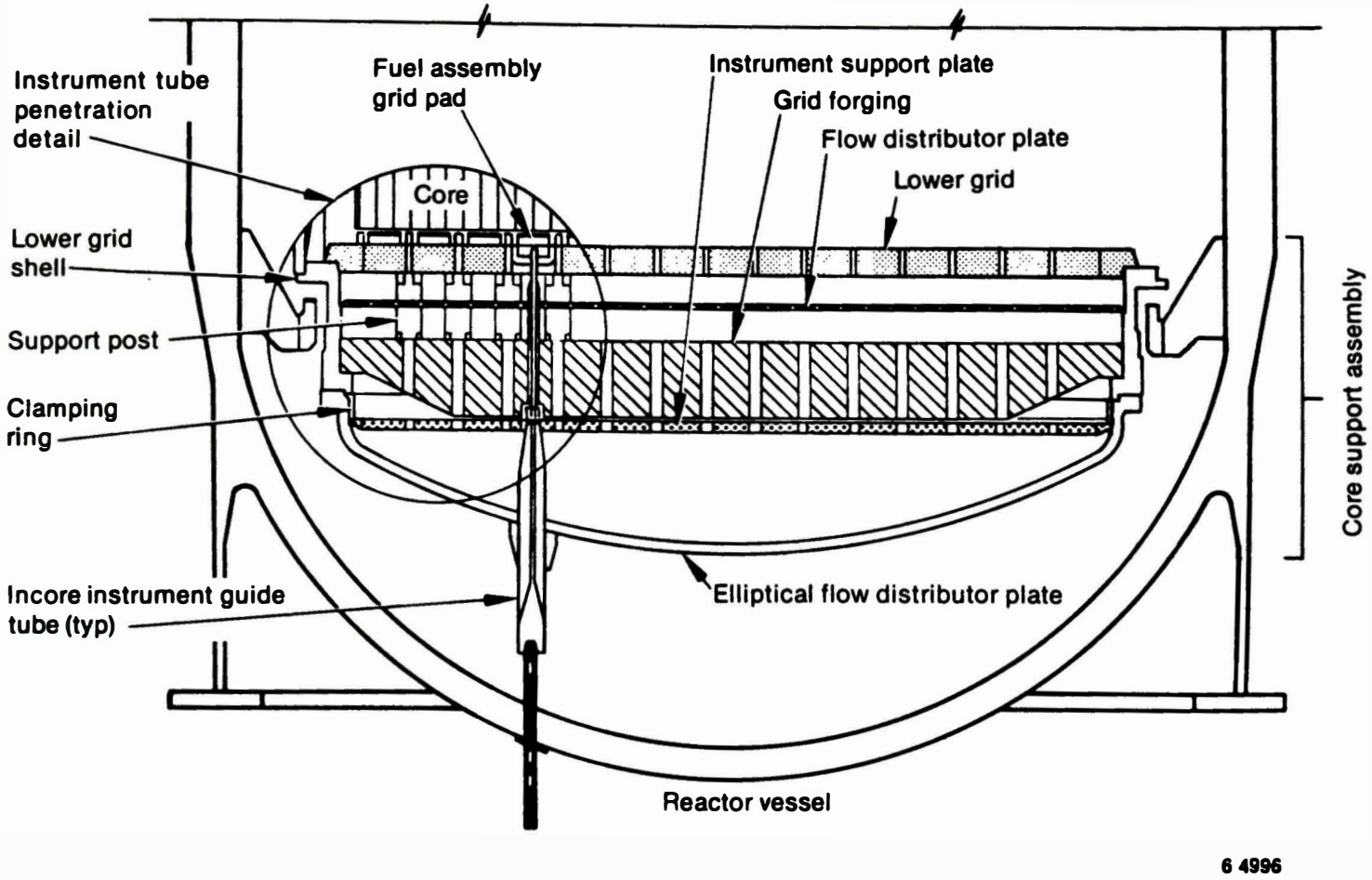

Figure 2. TMI-2 reactor vessel lower head and plenum.

instrumentation guide tube geometry in the lower plenum. These guide tubes were the principal fiducial points used in determining the debris bed depth at various locations. Appendix B summarizes the results from the lower plenum video inspection which was conducted in February, 1987, including photographs of the damaged instrument guide tube. While much of the visual data is of a qualitative nature, examination of these data has aided in development and confirmation of the accident scenario.[11]

TOPOGRAPHY

The volume and mass of the lower plenum debris bed are derived in this section. This was done by estimating the debris bed thickness at various locations, extrapolating these thickness estimates to the entire debris bed, and fitting contour lines to the bed, thus obtaining an estimate of the topography of the debris bed. Graphical sections of the debris bed at regular intervals were made, and the volumes for the sections were calculated and summed to derive the total debris bed volume. Finally, the total mass was derived using the debris bed volume and estimates of the debris packing fraction and density.

In some cases, the visual data were obscured, due to turbidity in the water. Because of this turbidity, as well as the limited extent of the visual examinations of the debris bed, there are areas of the bed where no depth measurements are possible. This is particularly true in the southeast quadrant of the lower plenum. The overall topography of the debris bed is therefore less certain than would be the case were the total debris bed available for inspection. This results in a concomitant increase in the uncertainty of the total debris bed volume and mass. Thus, the topography should be considered a "best effort;" and the estimate of total mass of corium in the lower plenum should be verified during the core removal operation.

Figure 3 shows the measured and estimated lower plenum debris bed depths as derived from the video data. The core grid is superimposed for reference. The debris bed depth data shown in Figure 3 were estimated using two techniques. For those locations examined using a camera inserted into the downcomer annulus, the debris bed height was estimated by comparing the top surface of the bed to the instrument guide tubes at various locations. The depth could then be estimated using the known geometry of these guide tubes. The detailed geometries of all guide tubes used in this study are shown in Appendix A. For the three lower plenum locations examined during the core-boring operations, grid locations K-9, D-4, and N-12, the camera was lowered to the top of the debris bed and then

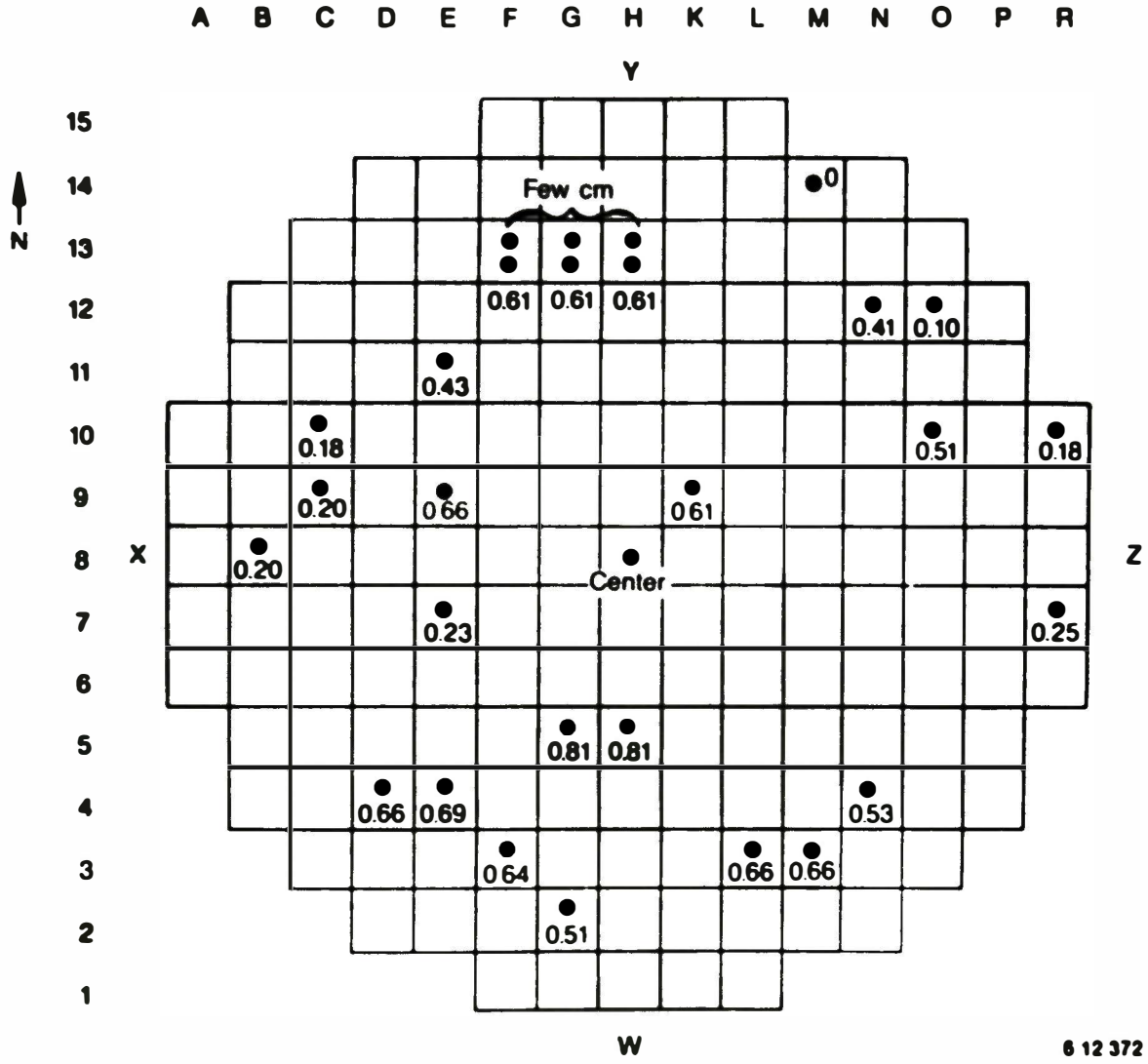

Figure 3. TMI-2 lower plenum debris bed depth measurements.

withdrawn to the bottom of the elliptical flow distributor plate, and the length of travel of the camera was measured. The debris bed depth at these three locations was then derived from the measured length of travel, using the known geometry of the lower head and elliptical flow distributor.

The contour lines for the spherical lower head of the reactor vessel were drawn using the design information for this component. These contours are shown in Figure 4, which is a plane view of the lower head with the core grid superimposed. The depth of the debris bed (at those locations shown in Figure 3) and the contour of the lower head were combined to provide estimates of the debris bed height above an arbitrary reference plane. The reference plane was chosen to intersect with the inside surface of the lower head at the reactor vessel centerline, the 290-ft, 11-in. elevation. These debris bed height estimates are shown in Figure 5.

Contour lines were drawn by manually interpolating between the debris bed height data. The manual contouring method is commonly used in geologic and topographic mapping and consists of the following. A contour interval is chosen, based on the range of elevations encompassed by the observation points. In this case, the contour interval was approximately 10 cm (4 in.). Then, contour lines are drawn, using the observation points as controls on the contour line positions and spacing. The resulting continuous surface contour is strictly controlled by the observation points. The contour of the lower plenum debris bed, derived using this method, is shown in Figure 6, which also includes the debris bed height estimates from Figure 5 for comparison.

As shown in Figure 6, the rubble bed extends to near the reactor vessel wall along three axes (W, X, and Z) but only to the last row of instrument guide tubes at the Y axis. This is illustrated by Figures 7 and 8, which are photographs of the lower rubble bed at the W and Y axes, respectively. The abrupt "wall" of debris at the Y axis is evident from Figure 8, while the rubble continues to the downcomer wall at the W axis shown in Figure 7. The top surface of the bed slopes from south to north, with a rounded depression extending from west to east in the central zone.

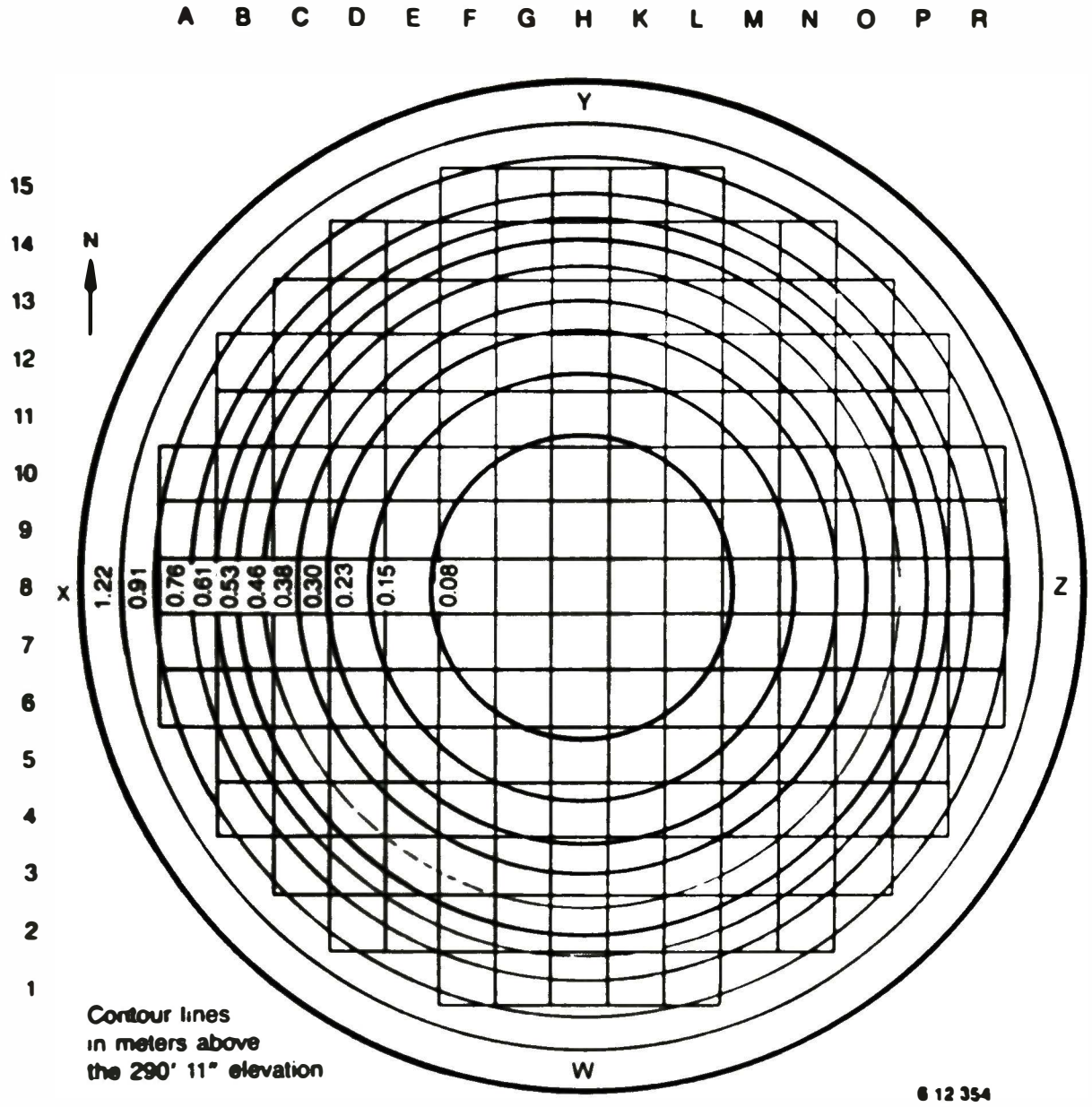

Figure 4. TMI-2 reactor vessel lower head contour map.

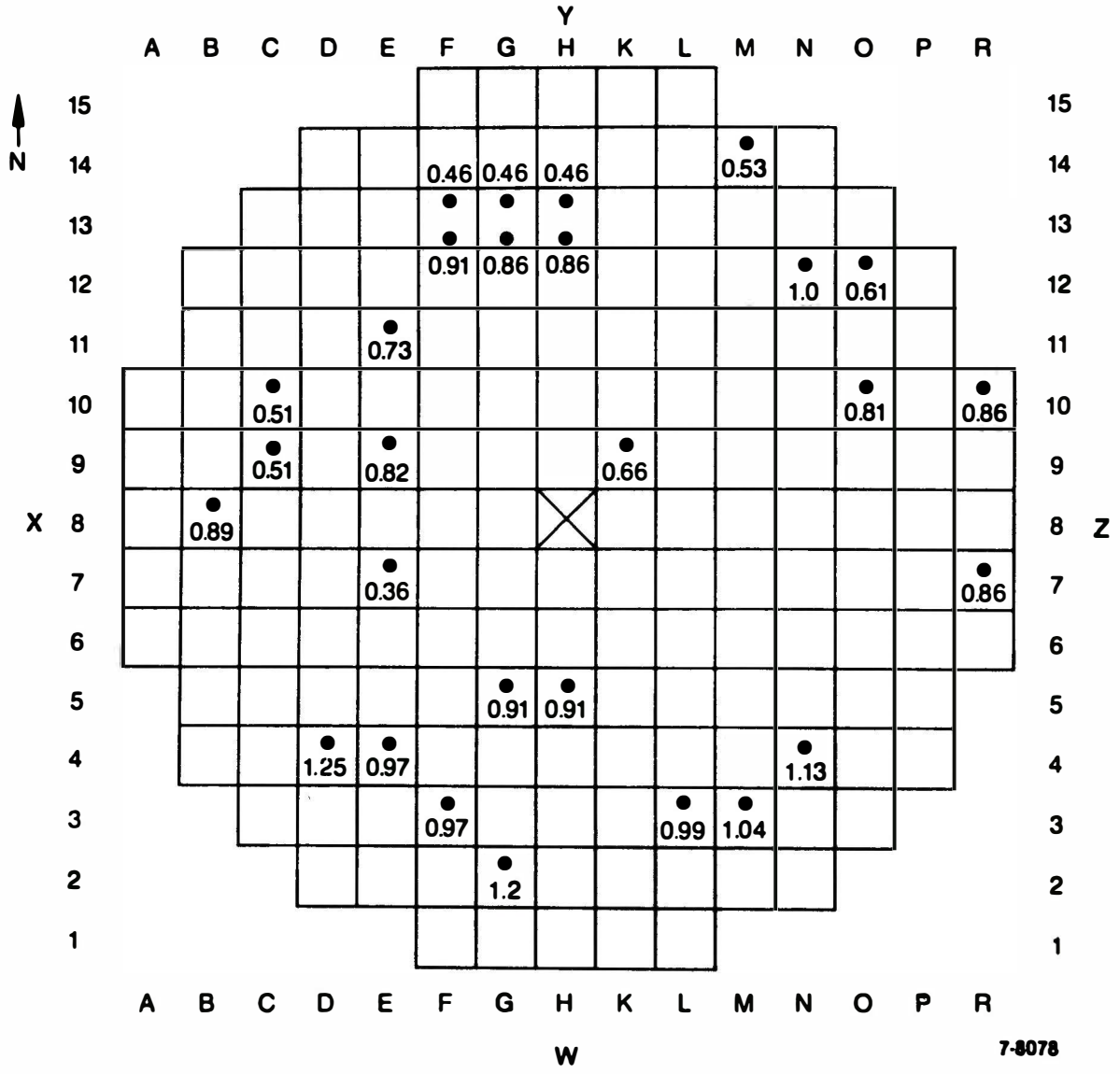

Figure 5. TMI-2 lower plenum debris bed surface.

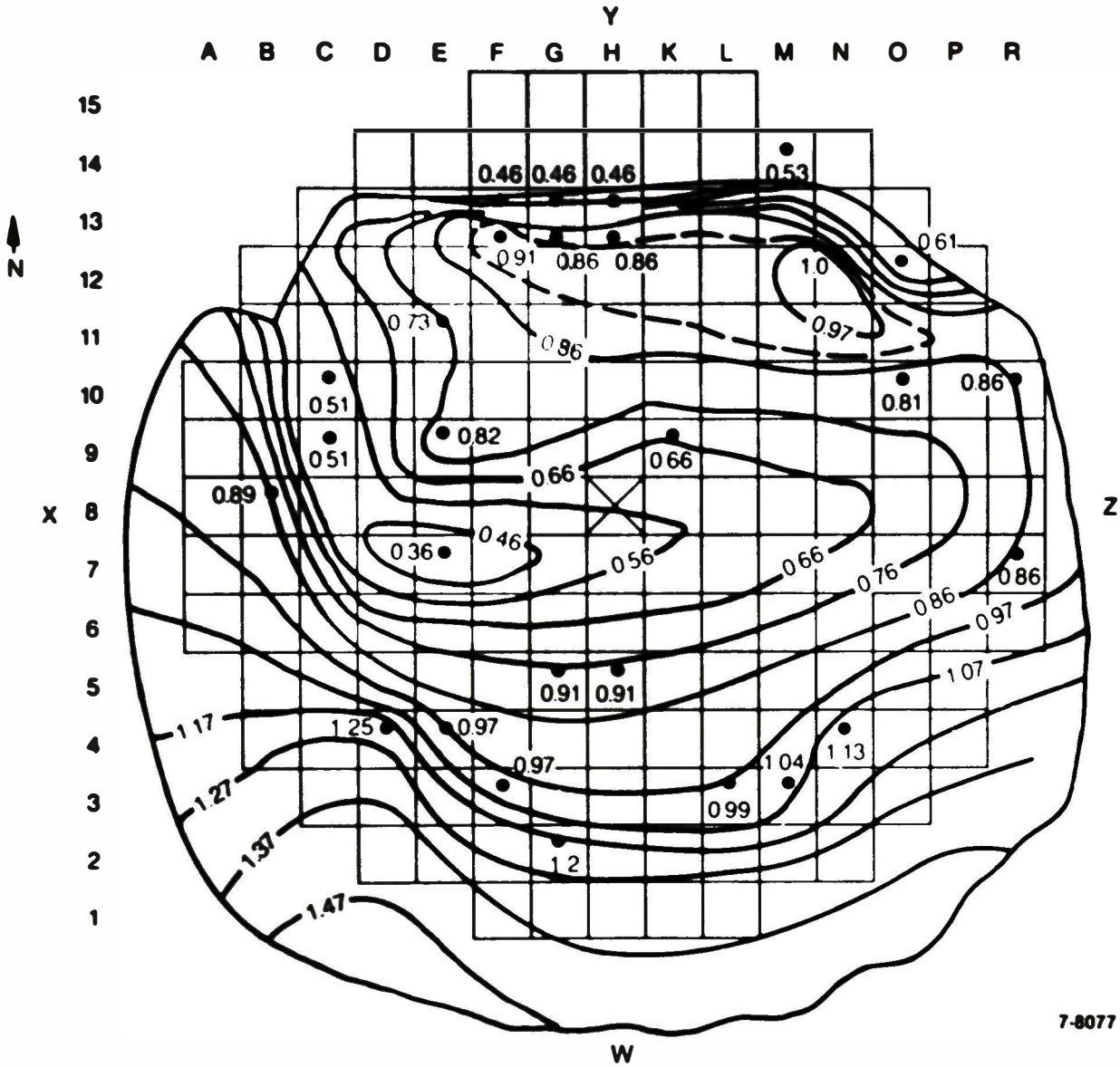

Figure 6. TMI-2 lower plenum debris bed contour map.

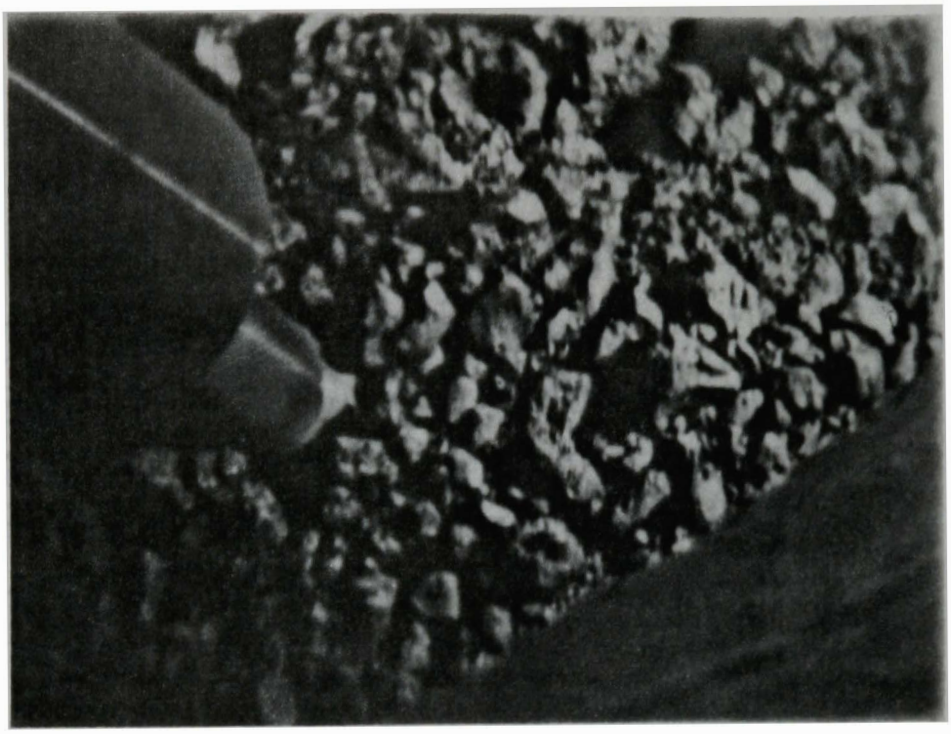

Figure 7. Photograph of TMI-2 lower plenum rubble bed at W axis.

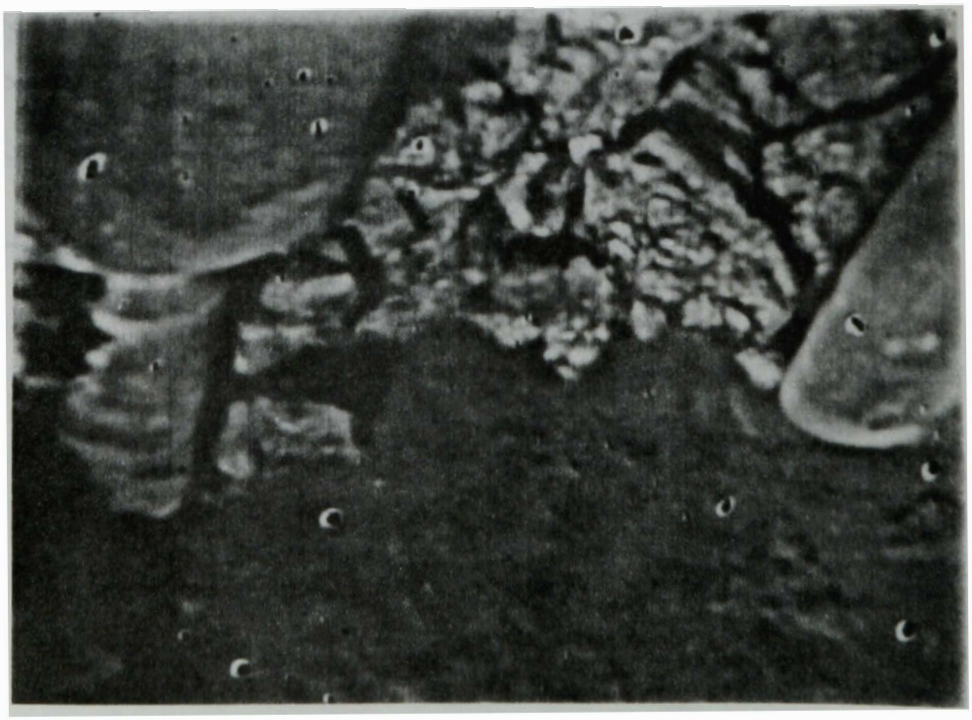

Figure 8. Photograph of TMI-2 lower plenum rubble bed at Y axis.

A total of 17 cross sections of the debris bed were made, one for each lettered row associated with the core grid plus one on each side to account for the debris which extended beyond the grid. The latter sections are labeled "AA" and "S." These cross sections were derived from contours of the debris bed (Figure 6) and the lower head (Figure 3) and are shown in Figures 9 through 25. The cross-sectional debris bed area was measured for each figure using a planimeter and was then multiplied by the cross-section thickness (0.22 m) to derive the associated volume. The area and volume for each cross section are listed in Table 1.

The mass of the debris in the lower plenum has been estimated by multiplying the debris bed volume by the debris bed density and packing fraction. The debris density used in this analysis was 7.00 ± 0.57 g/cm^3 and was based on the average of the densities of eight samples taken from the debris bed.[12] It was assumed in this analysis that the average debris density in the lower plenum was equal to the average from this very limited sampling. This assumption is, of course, not verified which adds an additional, unquantified uncertainty to the debris bed mass estimate.

There is no practical method for directly measuring the packing fraction (that fraction of the volume of the debris bed that is occupied by debris, as opposed to the fraction occupied by water) of the debris in the lower plenum. Therefore, only a rough estimate can be made of this quantity. An analysis of the packing fraction of the TMI-2 upper core debris bed was made by Moore.[13] In this analysis, a particle size distribution was assumed based on that measured in an out-of-pile experiment performed at the Kerforschungszentrum Karlsruhe;[14] these particles were allowed to settle, via computer simulation, onto the remaining fuel rod stubs. A few sensitivity calculations were made which estimated the dependency of the packing fraction to particle size distribution and vibrations. The range of packing fractions calculated for these conditions was 0.3 to 0.5, with the upper value corresponding to vibration-assisted settling. These values were compared with the packing fractions associated with loosely packed gravel, equal to 0.45. This

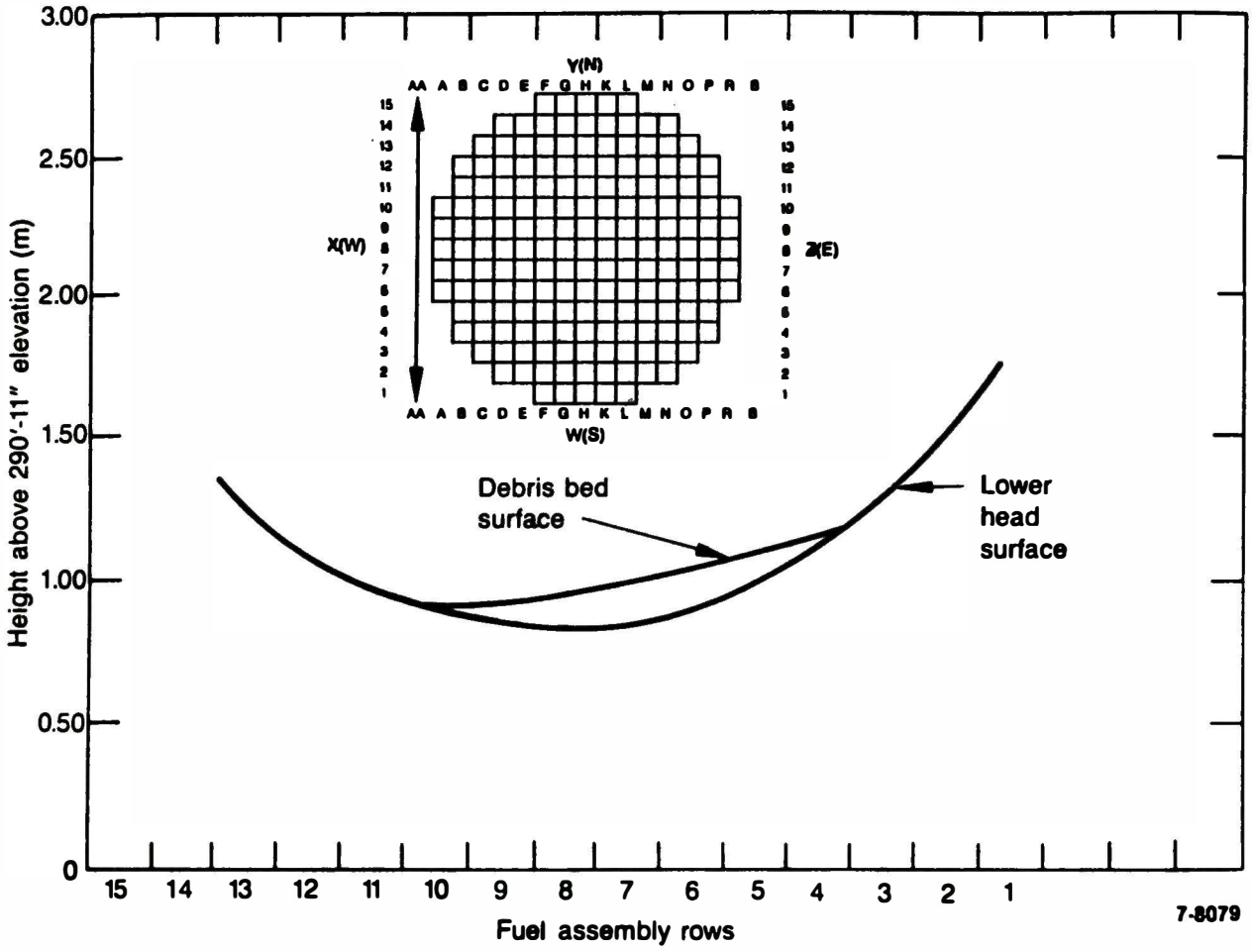

Figure 9. TMI-2 lower plenum debris bed estimated volume at Column AA based on contour map.

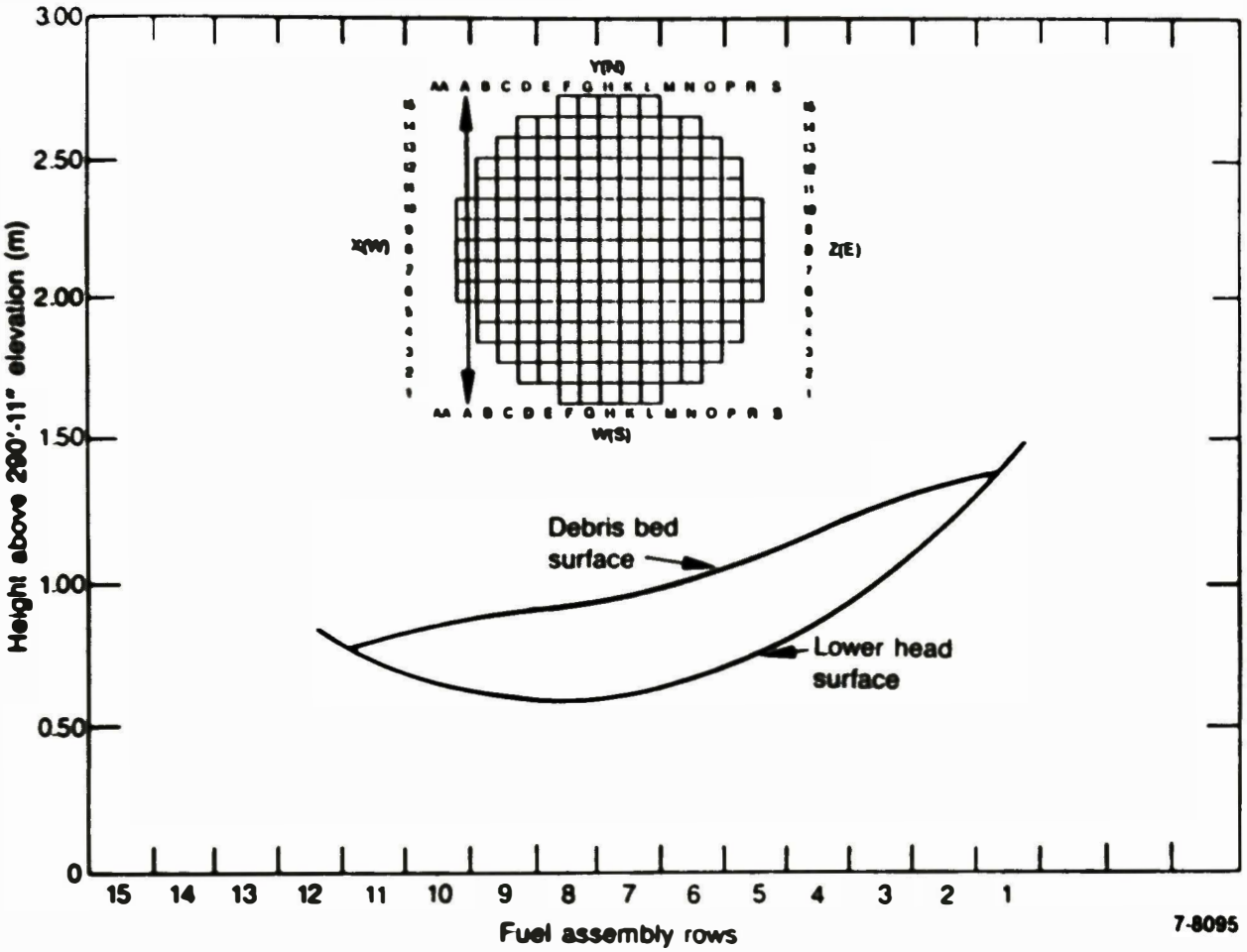

Figure 10. TMI-2 lower plenum debris bed estimated volume at Column A based on contour map.

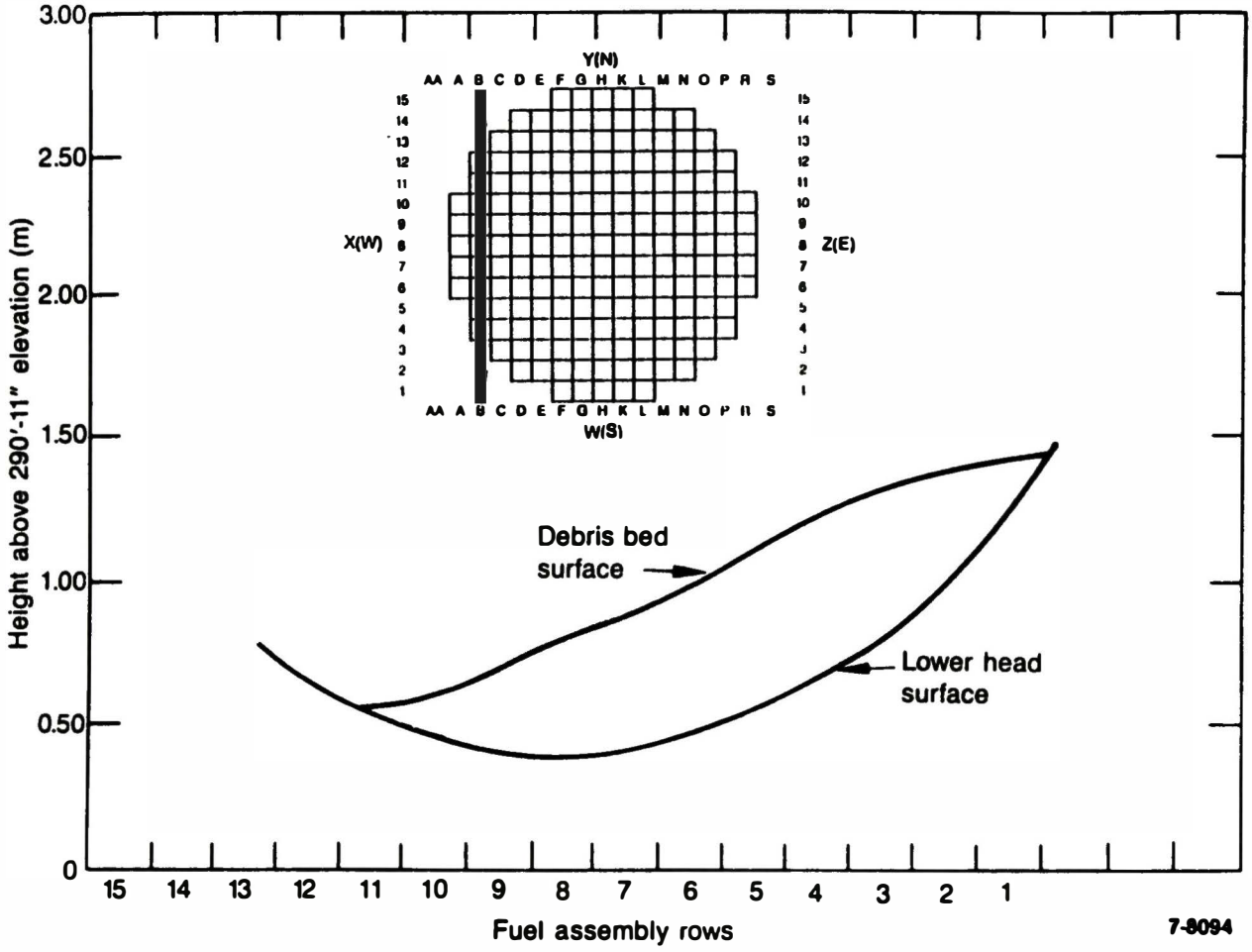

Figure 11. TMI-2 lower plenum debris bed estimated volume at Column B based on contour map.

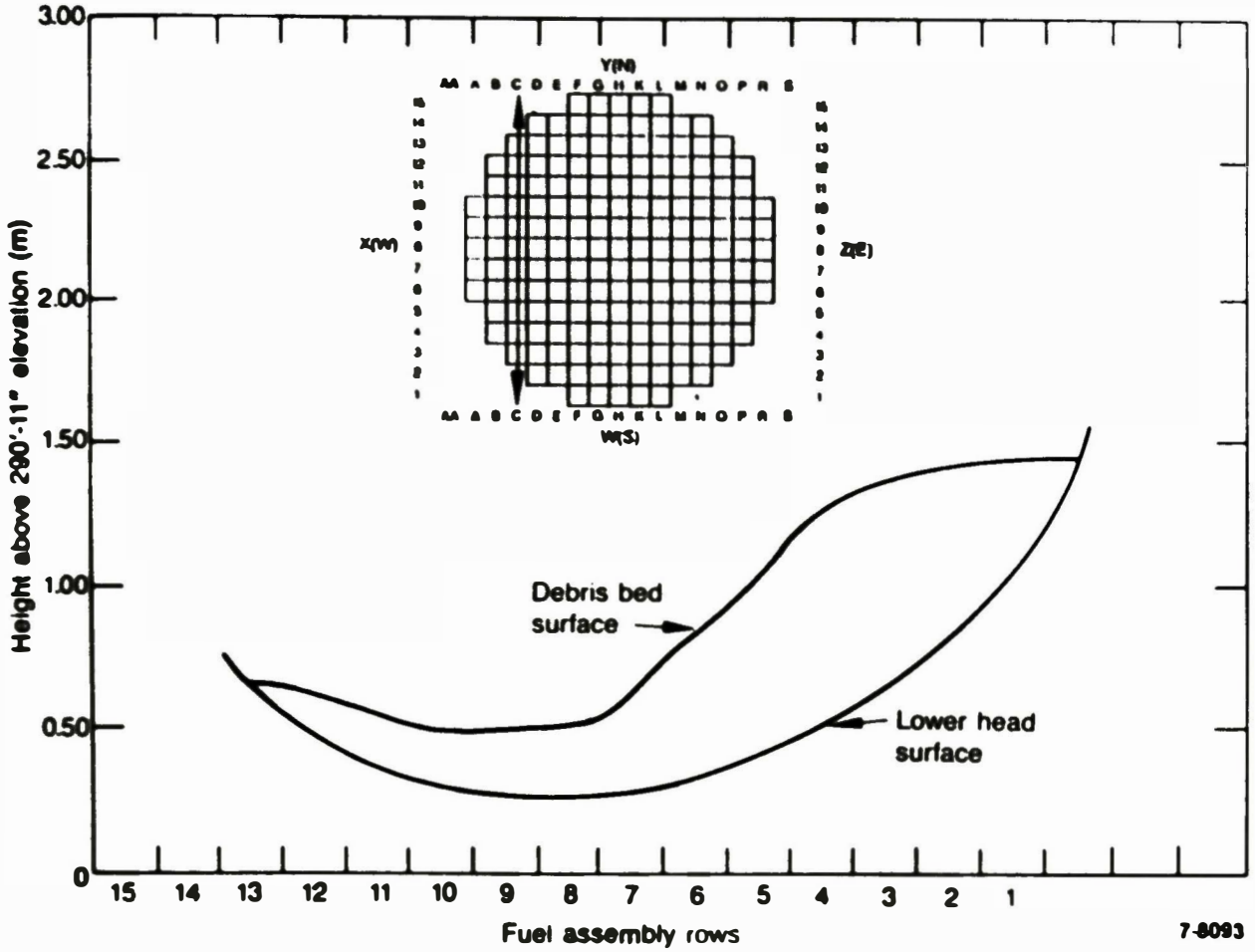

Figure 12. TMI-2 lower plenum debris bed estimated volume at Column C based on contour map.

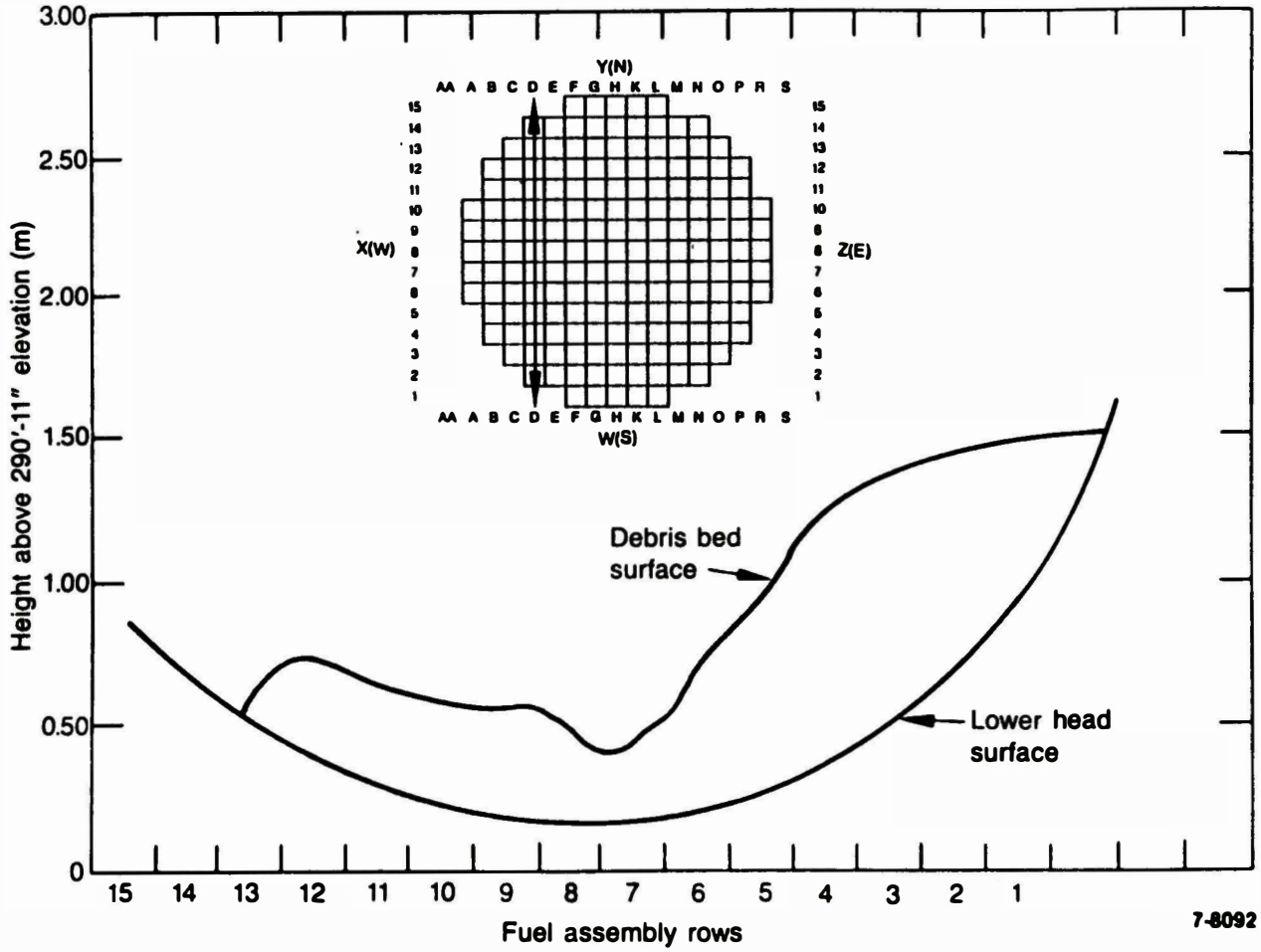

Figure 13. TMI-2 lower plenum debris bed estimated volume at Column D based on contour map.

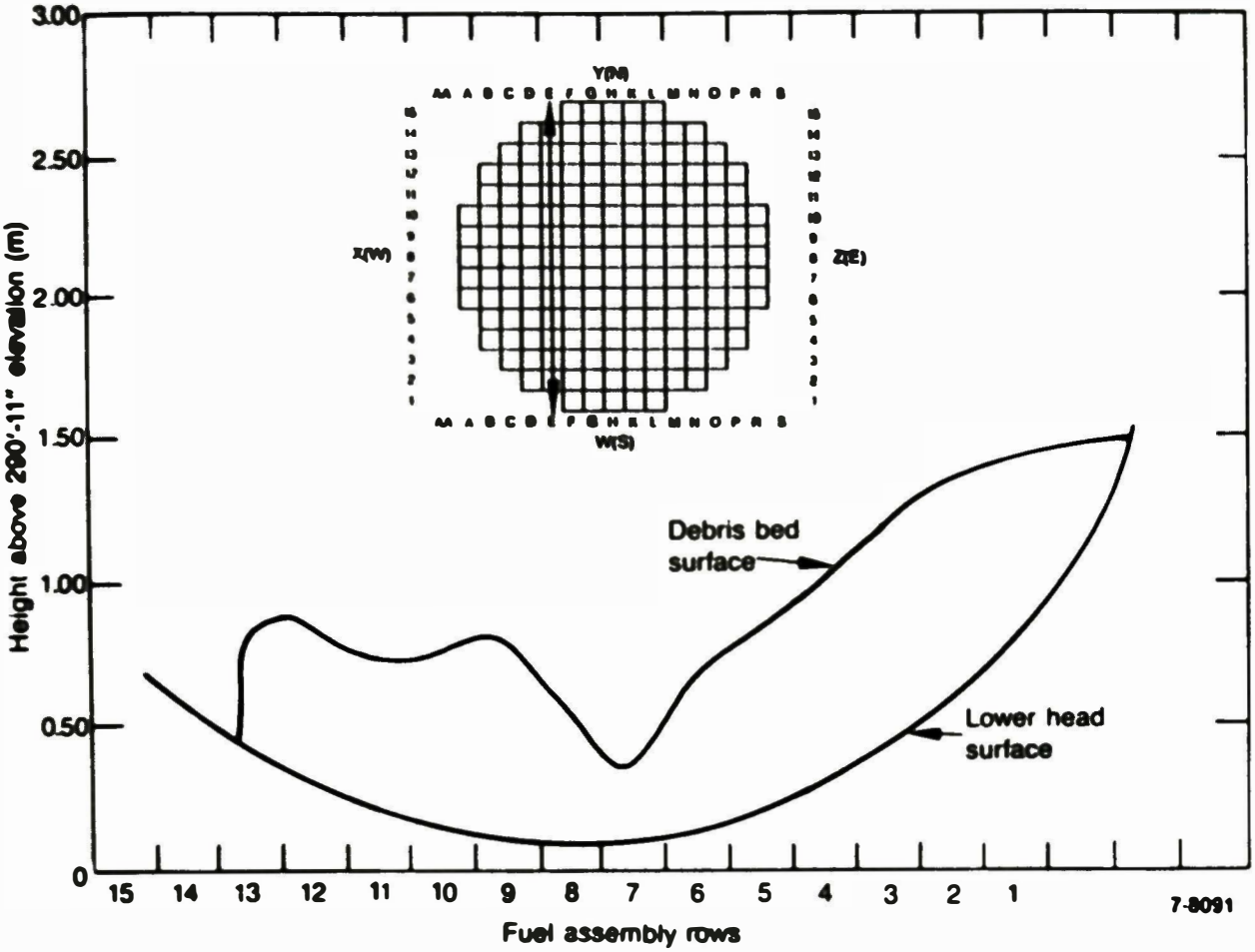

Figure 14. TMI-2 lower plenum debris bed estimated volume at Column E based on contour map.

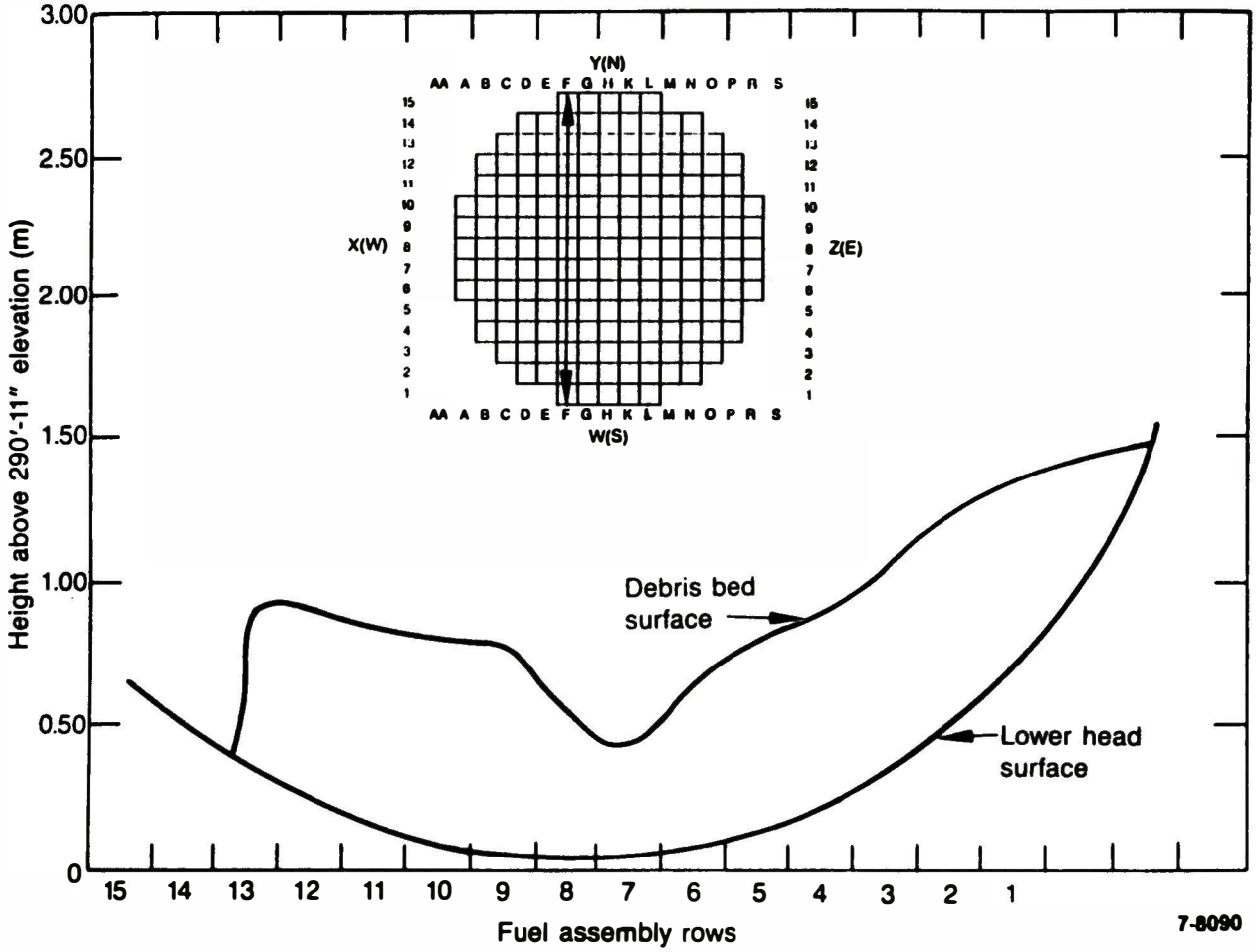

Figure 15. TMI-2 lower plenum debris bed estimated volume at Column F based on contour map.

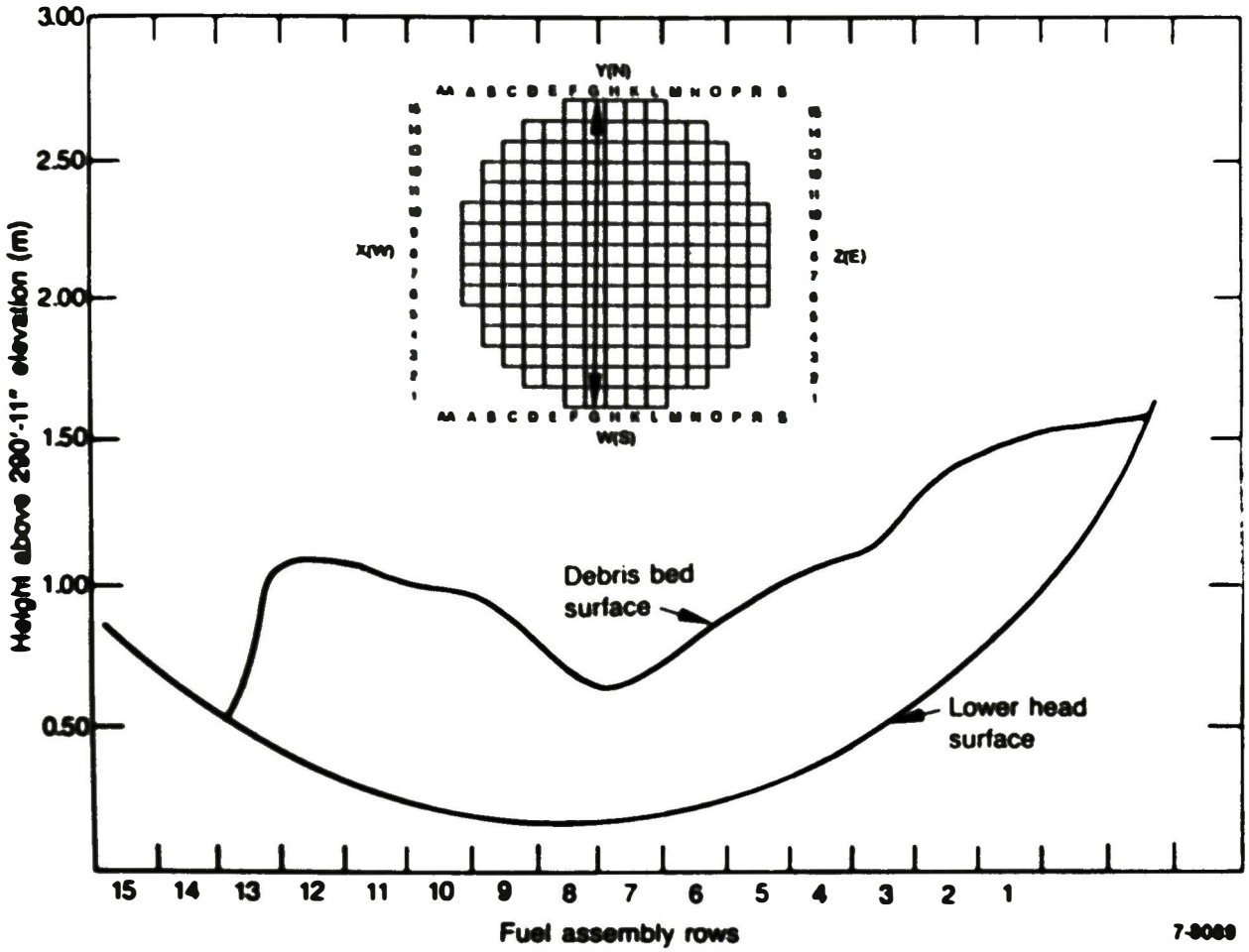

Figure 16. TMI-2 lower plenum debris bed estimated volume at Column G based on contour map.

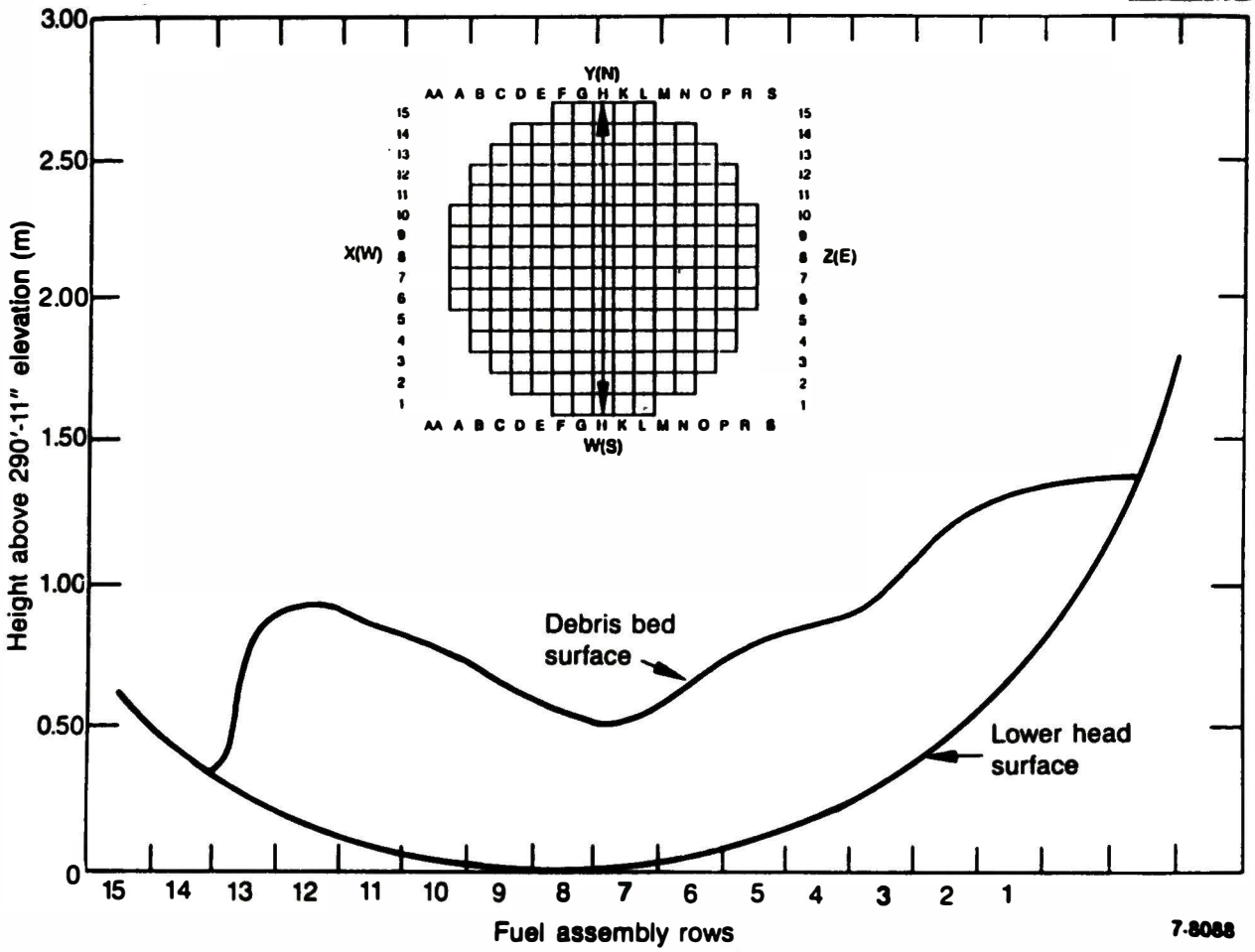

Figure 17. TMI-2 lower plenum debris bed estimated volume at Column H based on contour map.

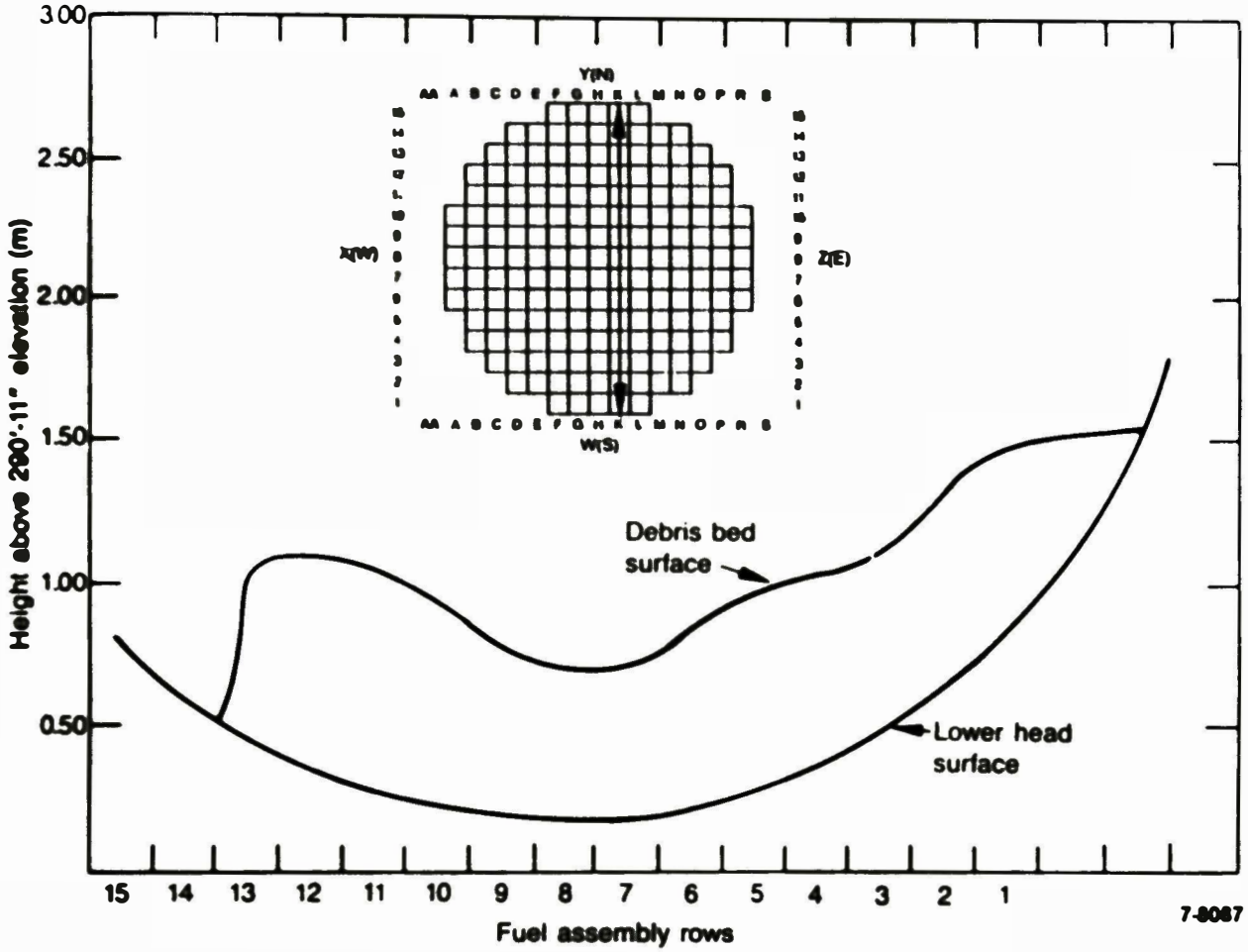

Figure 18. TMI-2 lower plenum debris bed estimated volume at Column K based on contour map.

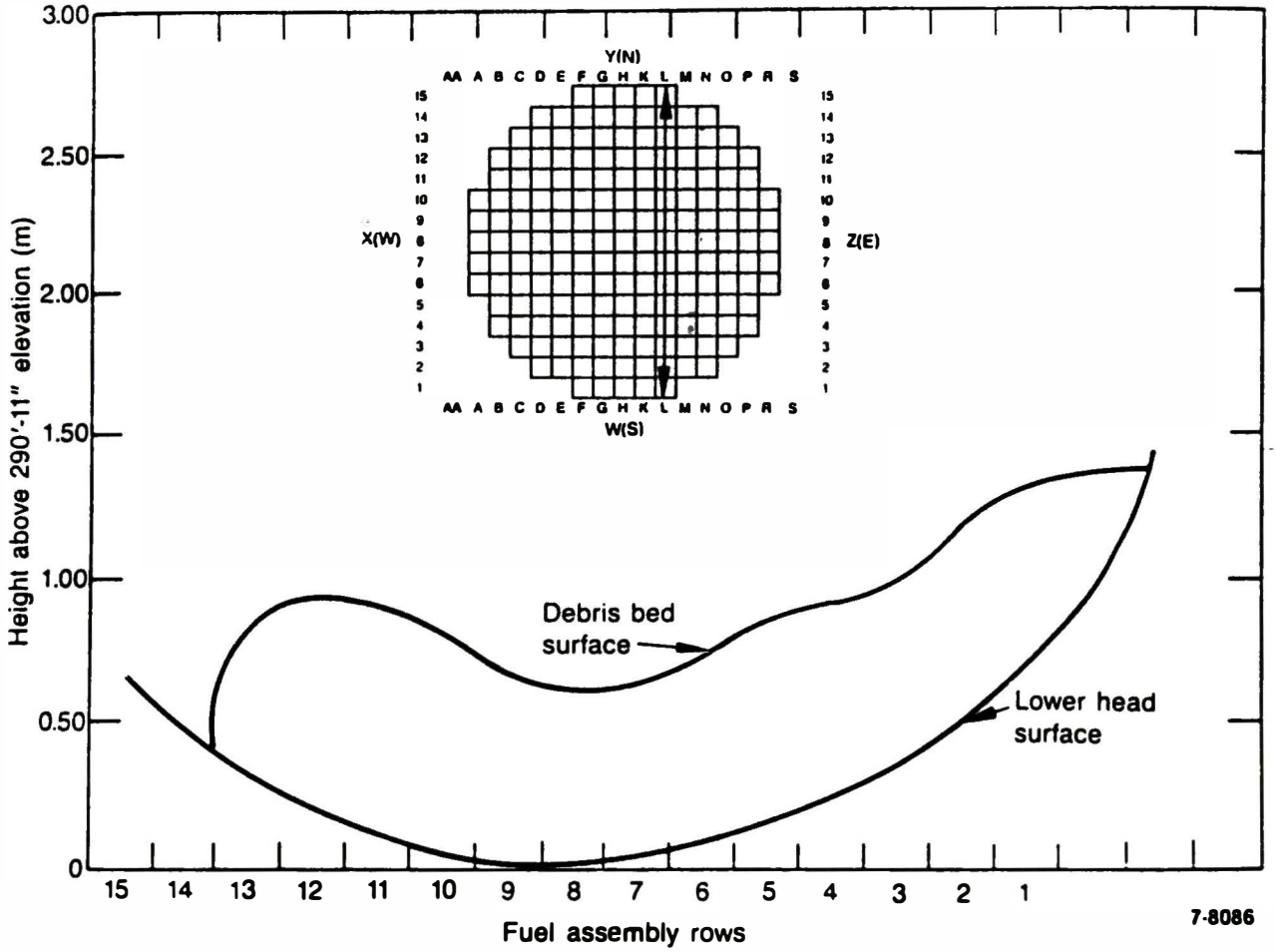

Figure 19. TMI-2 lower plenum debris bed estimated volume at Column L based on contour map.

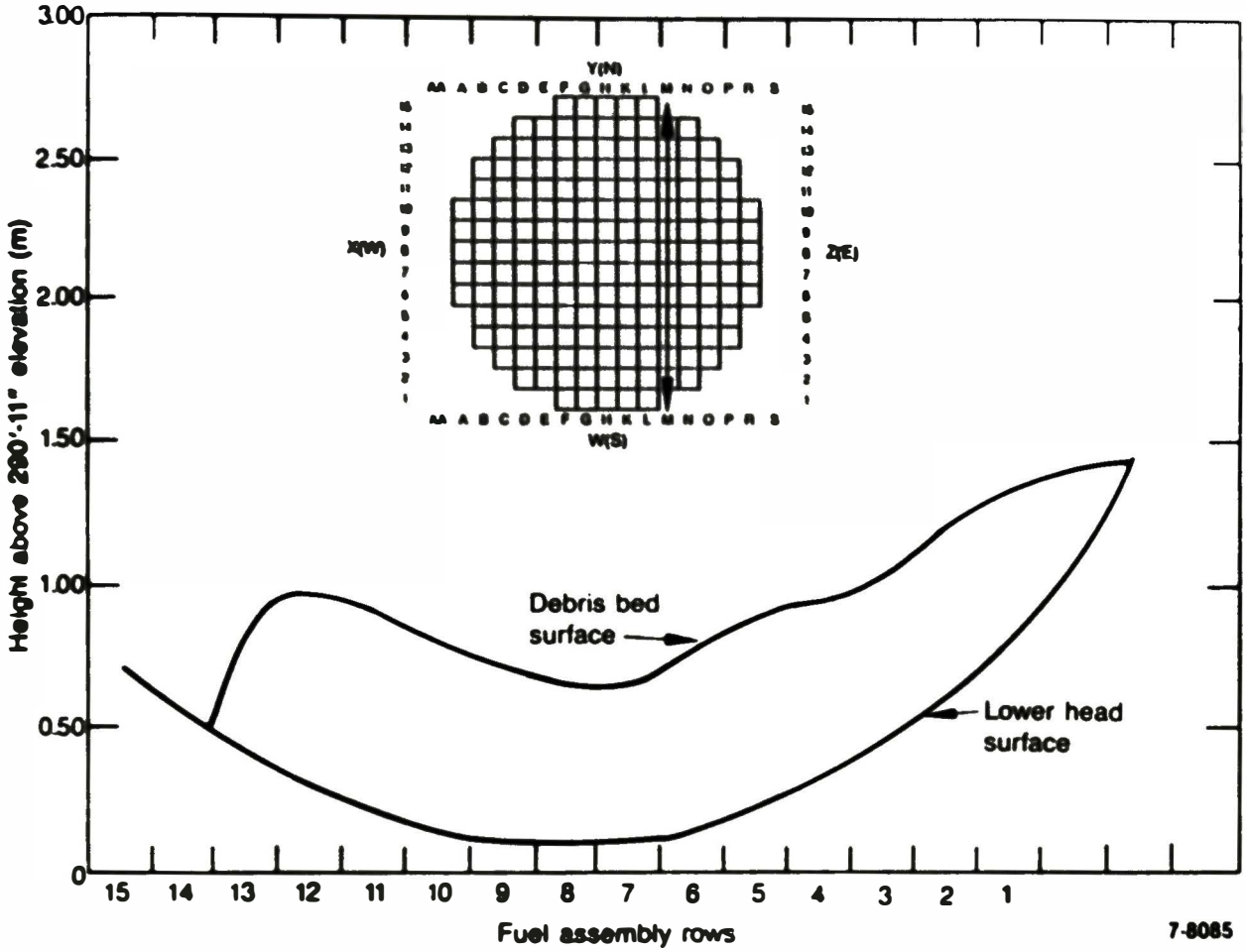

Figure 20. TMI-2 lower plenum debris bed estimated volume at Column M based on contour map.

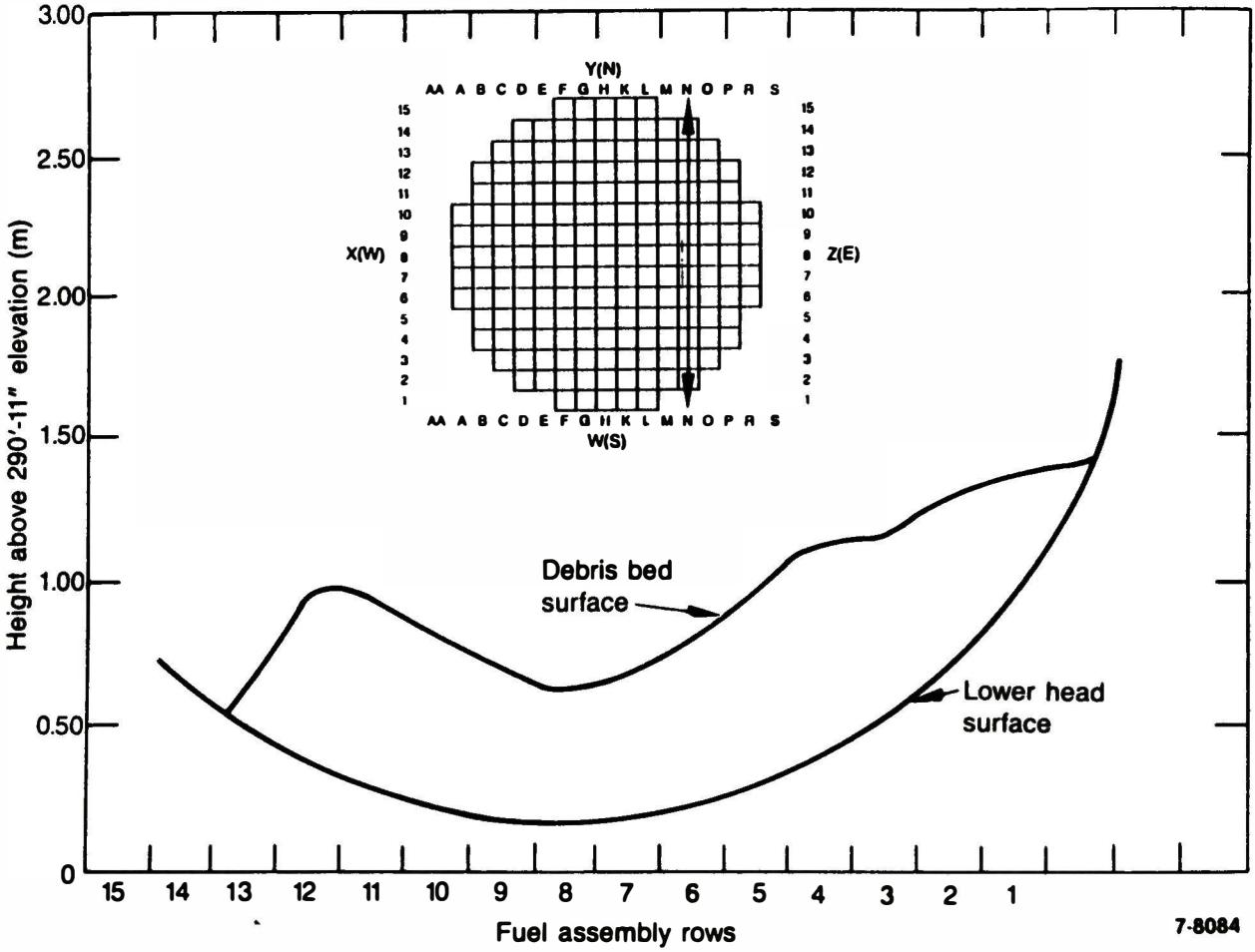

Figure 21. TMI-2 lower plenum debris bed estimated volume at Column N based on contour map.

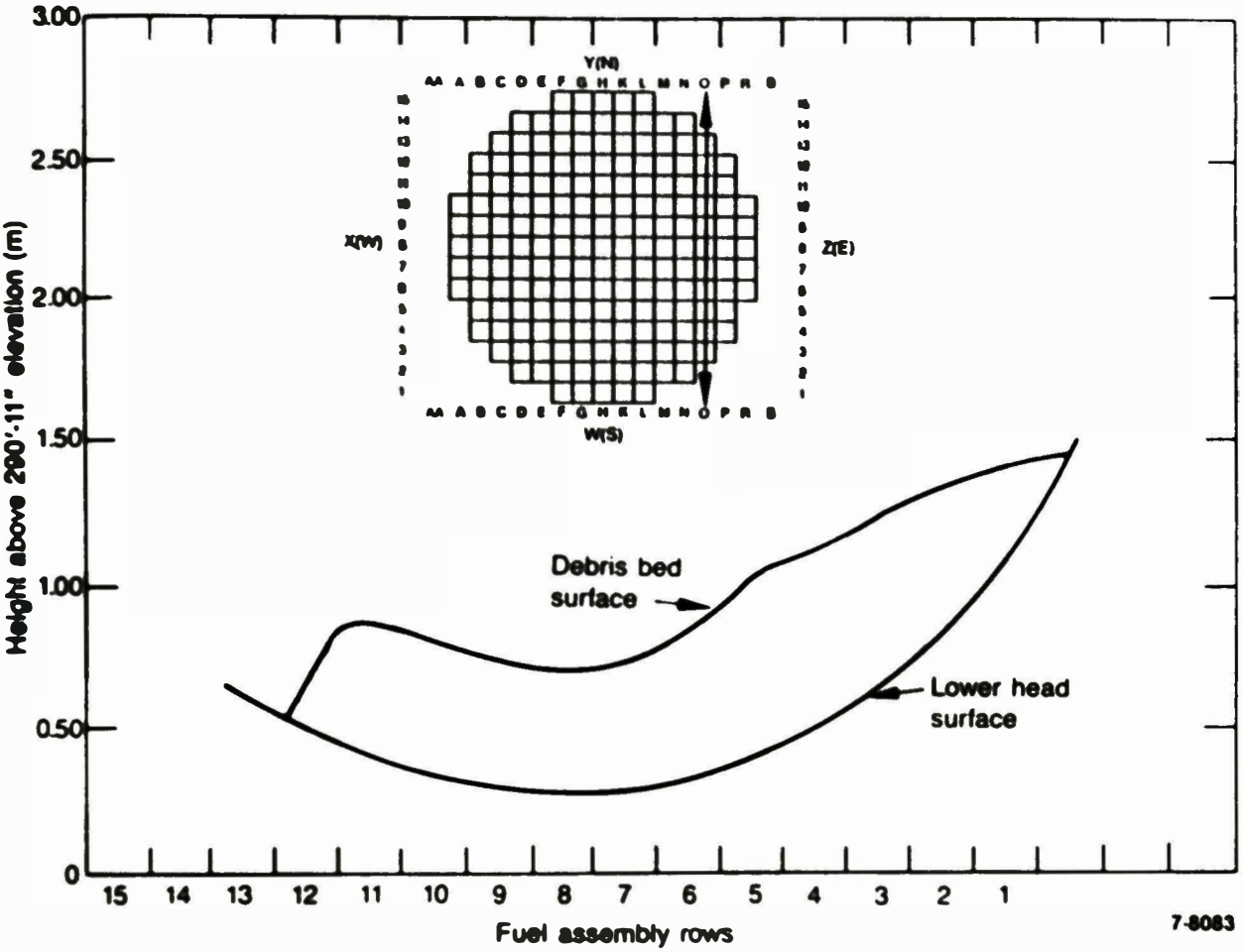

Figure 22. TMI-2 lower plenum debris bed estimated volume at Column O based on contour map.

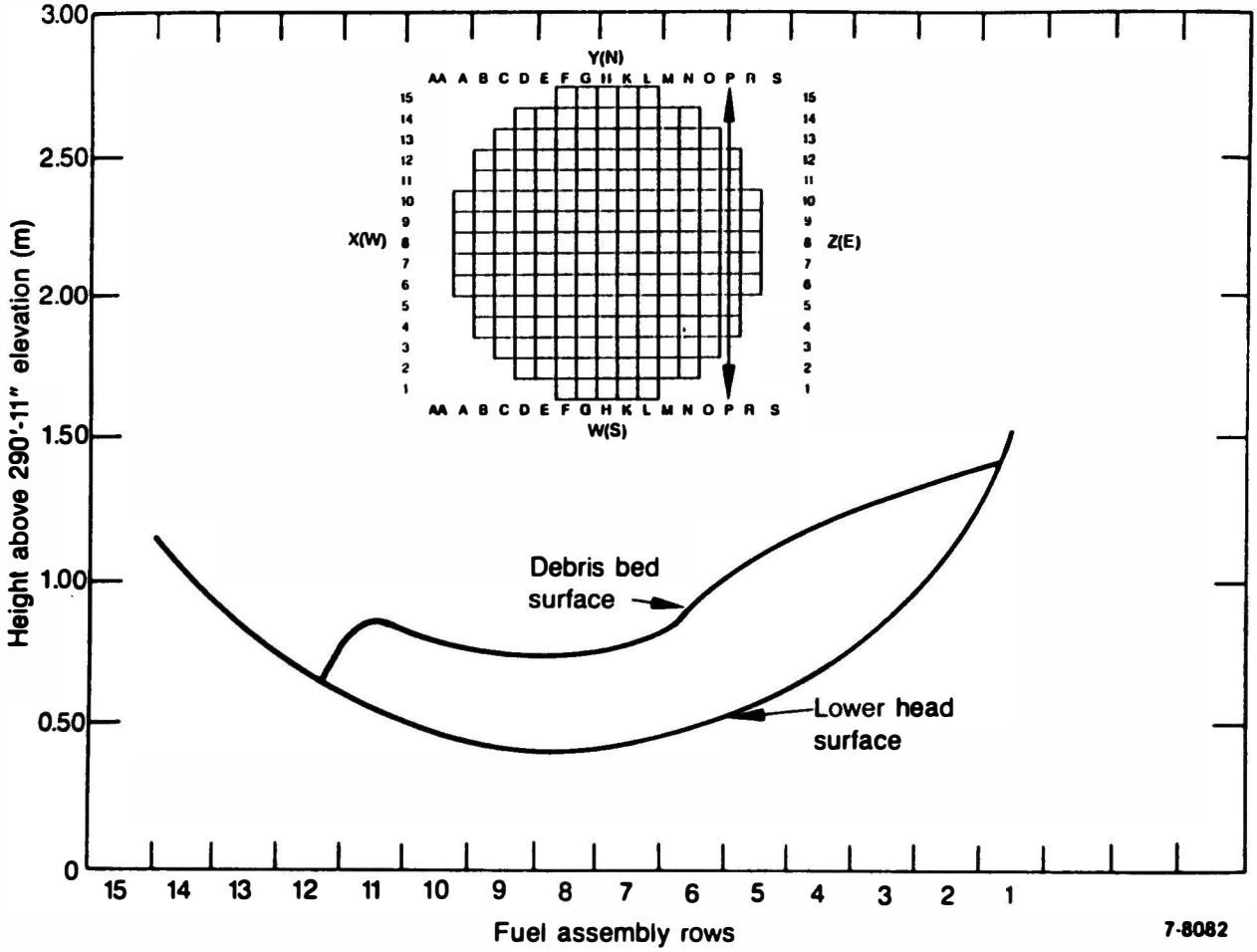

Figure 23. TMI-2 lower plenum debris bed estimated volume at Column P based on contour map.

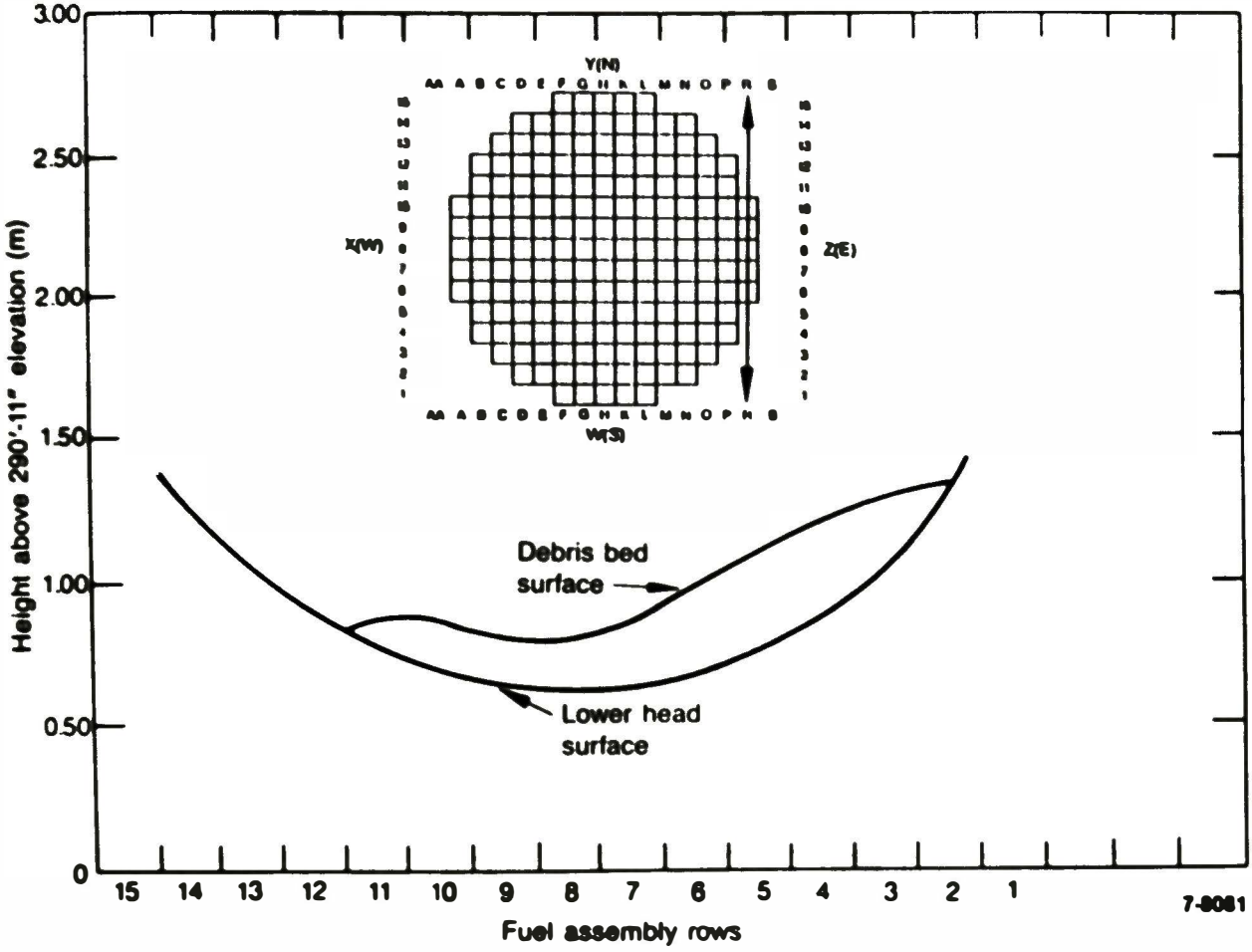

Figure 24. TMI-2 lower plenum debris bed estimated volume at Column R based on contour map.

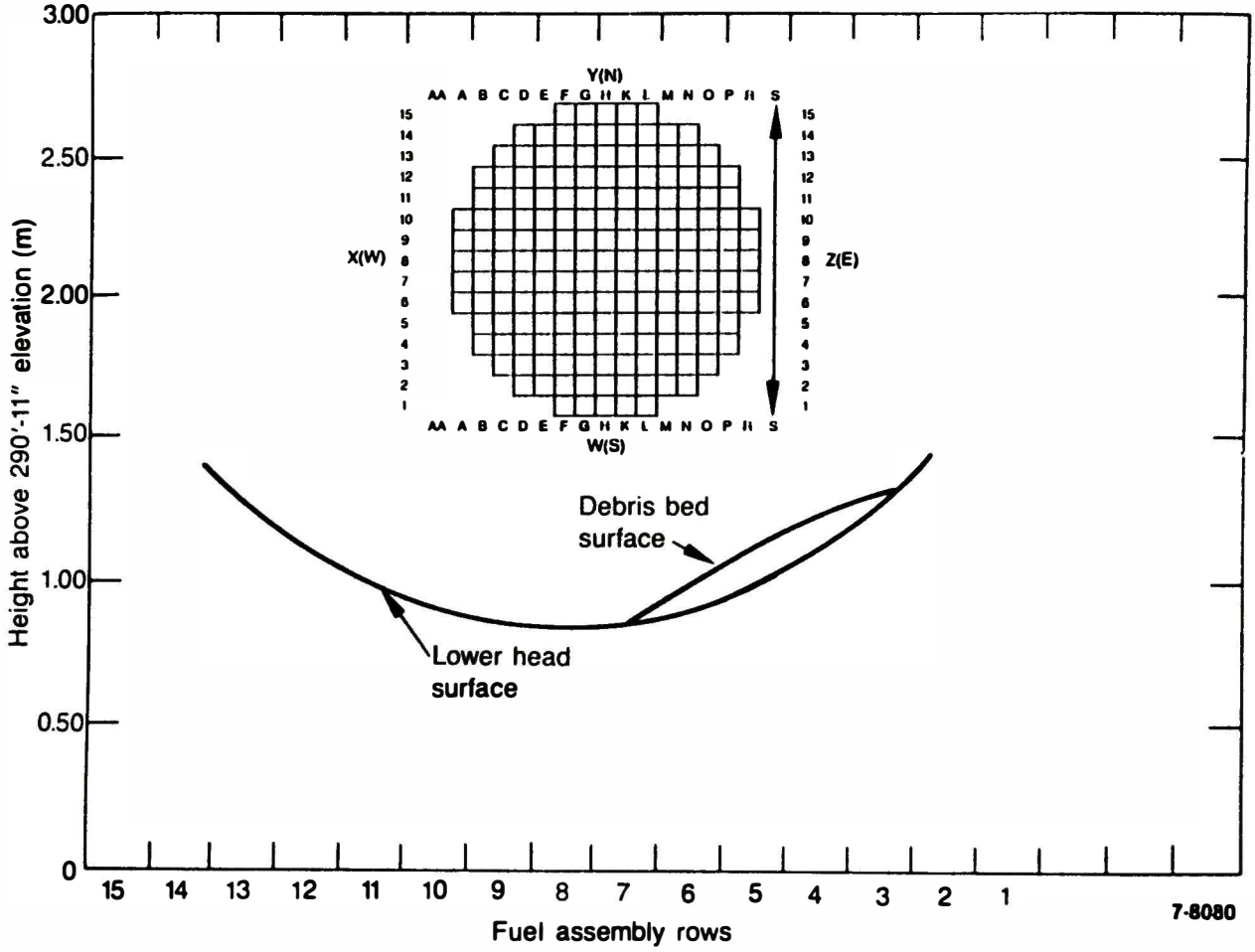

Figure 25. TMI-2 lower plenum debris bed estimated volume at Column S based on contour map.

TABLE 1. TMI-2 LOWER PLENUM DEBRIS VOLUME

Section	Area (m^2)	Volume (m^3)
AA	0.16	0.03
A	0.50	0.11
B	0.82	0.20
C	1.02	0.22
D	1.53	0.33
E	1.78	0.39
F	1.93	0.42
G	2.07	0.45
H	2.05	0.46
K	2.12	0.46
L	1.98	0.43
M	1.88	0.41
N	1.58	0.35
O	1.30	0.28
P	0.88	0.19
R	0.47	0.10
S	0.09	0.02
Total volume		4.85

analysis does not apply directly to the lower plenum debris bed because of several differences between the two debris beds, e.g., different temperature histories leading to differences in chemical and physical composition, fuel rod stubs in the upper debris bed, differences in the effects of postaccident reactor coolant pump operations, etc. However, the similarity of the results to that measured for a loosely packed gravel bed gave some credence to using these results as an estimate for the lower plenum debris bed. Thus, the value of 0.45 was used to estimate the mass of the lower plenum debris bed with an uncertainty of ±0.1.

Combining these three estimates (4.85 m^3 for volume, 7.00 g/cm^3 for density, and 0.45 for packing fraction) results in an estimated mass of 15 metric tons. Reference 9 states that the debris bed mass is 19.3 metric tons, based on an analysis of the response of the source range monitor.

A rigorous uncertainty analysis has not been performed for the mass of the lower plenum debris bed. However, it is judged that this uncertainty is of the order of 34% based on the following. The total debris bed volume is 4.85 m^3, based on the summation of the cross-section volumes listed in Table 1. The data used in deriving the topography of the lower plenum debris bed were those considered to be reliable and have an estimated uncertainty of 1 to 2 in. The exceptions to this are the data from the core bore inspections, which have an uncertainty of 3 to 5 in., and the three data points at grid locations F-13, G-13, and H-13, which have a higher, unquantified uncertainty. These three latter data points were used, in spite of their large uncertainty, because they represent the presence of a "wall" of debris at these locations, a structure which has been confirmed by the video data. An earlier topographical analysis was performed using additional, less reliable, data points in the southeast quadrant as well as data points which have since been determined to be incorrect. The debris bed volume, as determined in this previous topographical analysis, was 4.03 m^3, or approximately 17% less than in the current analysis. This difference in volume estimates is a measure, albeit unrigorous, of the uncertainty in the topographical analysis method. The reported uncertainty has been arbitrarily increased to 25% to allow for other unquantifiable uncertainties in the method.

The uncertainty in the debris bed particle density was estimated earlier to be ±0.57 g/cm^3, or 8%. The uncertainty in the packing fraction was chosen to be ±0.1, or 22%, based on the upper debris bed packing fraction analysis and the packing fraction of loosely packed gravel. These uncertainties--25% for volume, 22% for packing fraction, and 8% for density--were combined to obtain an overall uncertainty in the debris bed mass of ±34%, or 5 metric tons. Thus, the debris bed mass is estimated to be 15 ± 5 metric tons, which agrees within uncertainty with the debris bed mass of 19.3 metric tons derived from analysis of the source range monitor response.

During the lower plenum inspection, debris was observed in some of the holes in the elliptical flow distributor head. The debris in this region was mainly observed during the February 1985 inspection of the Z axis (hole No. 4), the December 1985 inspection of the Y axis (hole No. 14), and the December 1985 inspection of the W axis (hole No. 7). The region of inspection (of the elliptical flow distributor head) was very limited, and no attempt has been made to map the region where debris has been observed. Enhanced photographs were made from the video tapes to illustrate this debris. Figures 26 through 28 are photographs of the debris in the flow holes at different locations. It should be emphasized that only a part of the flow distributor plate was examined due to the lack of a camera manipulator during some of the inspections. Also, since the core was broken up due to the drilling operations, causing additional debris to be relocated to the CSA, it will be difficult, if not impossible, to determine the condition of this head after the accident by additional inspections.

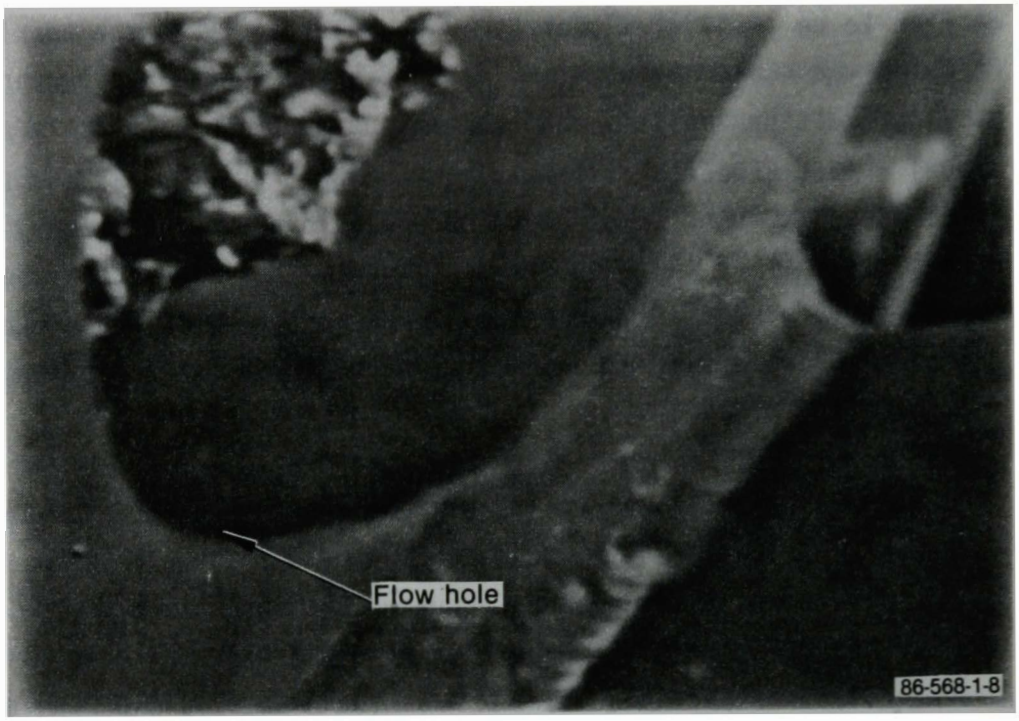

(a)

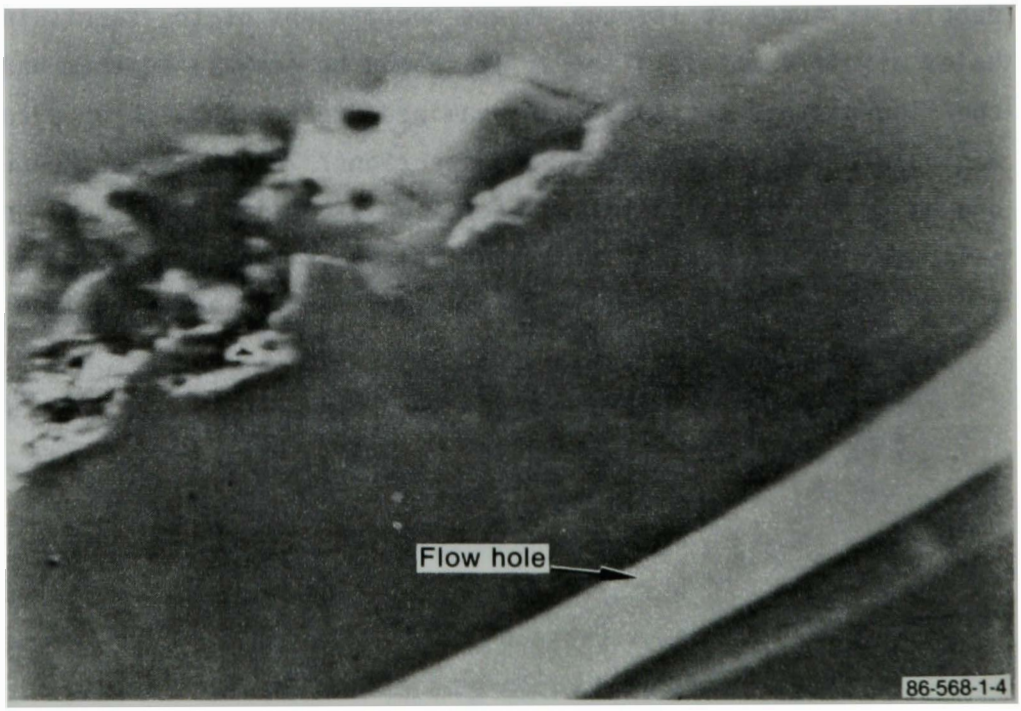

(b)

Figure 26. Photographs of TMI-2 debris in flow hole at Z axis.

(c)

Figure 26 (continued).

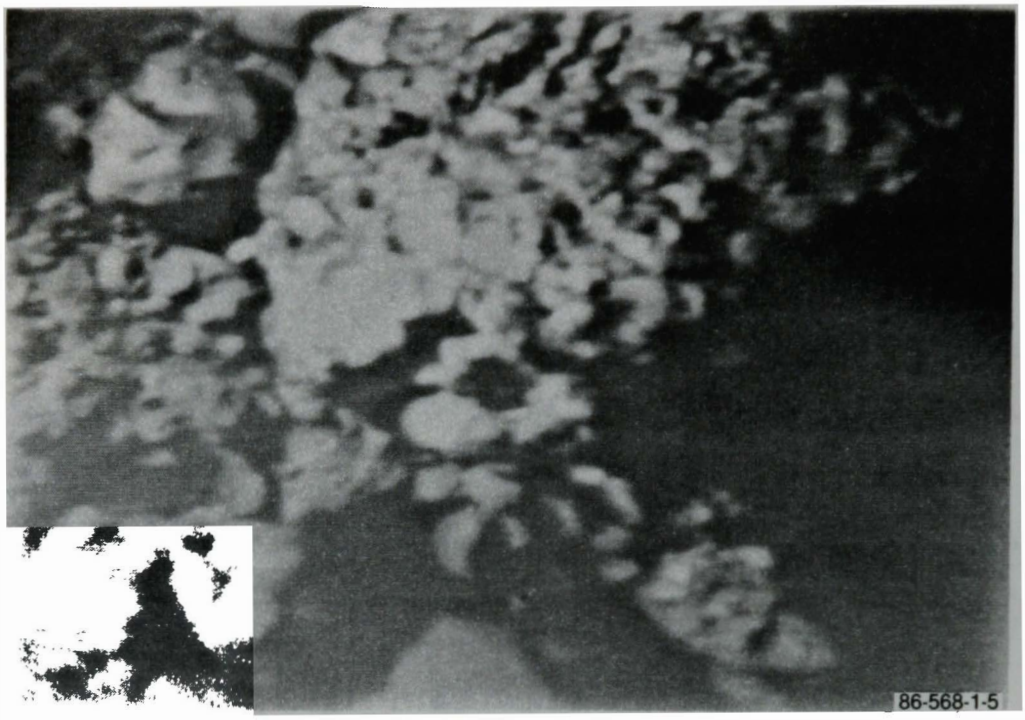

Figure 27. Photograph of TMI-2 debris on top of elliptical flow distributor plate.

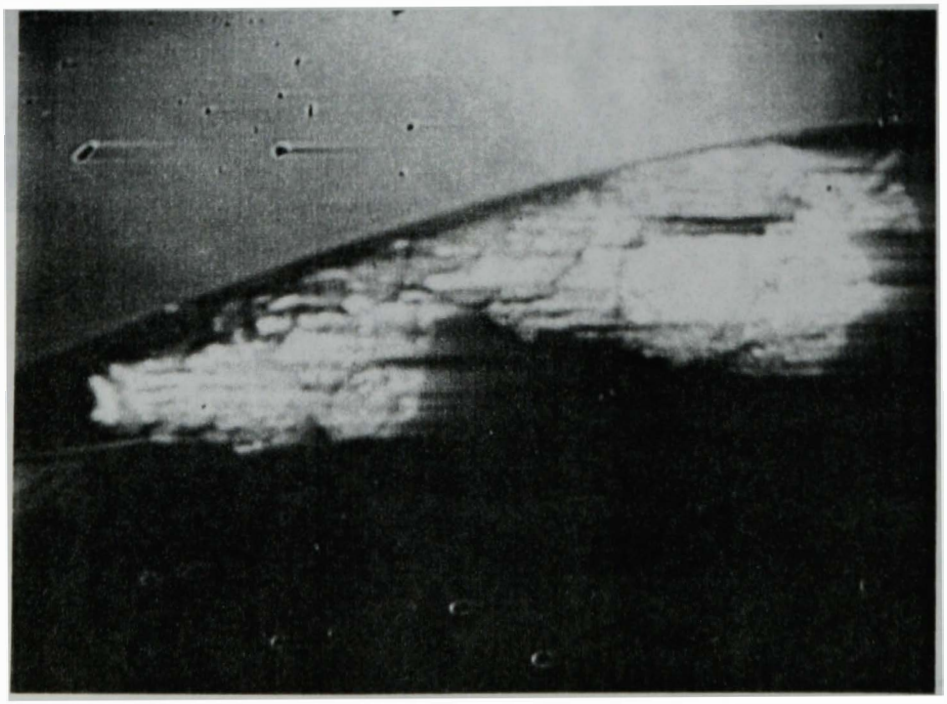

Figure 28. Photograph showing previously molten corium in flow hole at W axis.

RUBBLE BED COMPOSITION

Large differences in physical appearance exist in the rubble bed. The rubble near the Y axis, as indicated earlier, has the appearance of a large, lava-like cliff which abuts the outermost row of instrument guide tubes (see figure 8). The region in front of the rubble cliff has almost no debris. In some places, the lower head can be seen, indicating only a light "dusting" of debris at this location. The cliff appears to be solid with a smooth surface interlaced with cracks. There are also some large chunks of previously molten corium which may be loose.

The rubble near the X axis has a large number of 2- to 5-cm-sized chunks interspersed with much finer material. This is illustrated by the photograph of this area shown in figure 29.

The Z axis appeared to have the largest chunks. At least one chunk is estimated to be 15 to 20 cm in size. Several other large (7 cm or larger) chunks also are present. The larger pieces look porous, with small cracks and smooth surfaces. Figures 30 and 31 illustrate the coarseness of the debris bed in this region.

The W axis debris bed looks like a uniform bed of fine to medium-sized debris (see figure 7). A few larger chunks also exist, but the sizes of these chunks are not determined. There is a transition zone in this region, with a sharp transition between a very uniform and smooth rubble bed and a bed with a large number of medium-sized chunks. The rubble is easily dislodged by the camera and lights. Figures 32 and 33 are photographs of each side of this transition zone.

The rubble bed at all three core bore locations is very uniform and smooth with few, if any, large chunks. The chunks that are there appear to be small (1 to 2.5 cm in size) compared with those at the periphery of the lower plenum. However, the debris bed surface was perturbed by the additional debris that sifted down during the boring operation. Figure 34 is a photograph of the rubble bed taken during the core-boring operation at

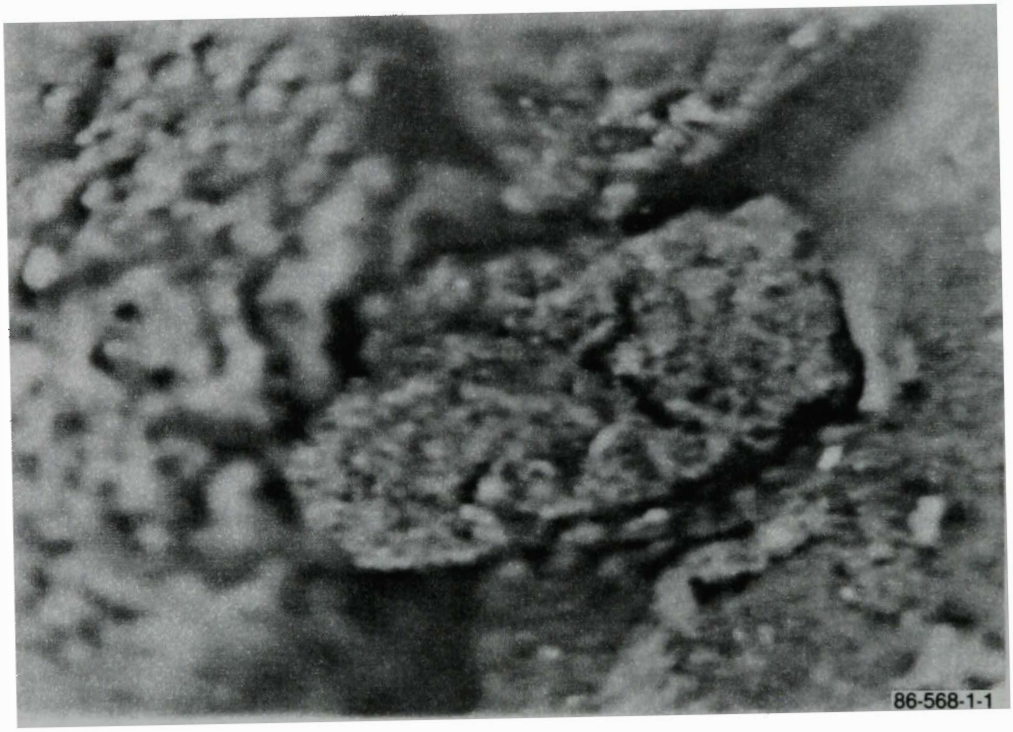

Figure 29. Photograph of large TMI-2 debris chunk at X axis.

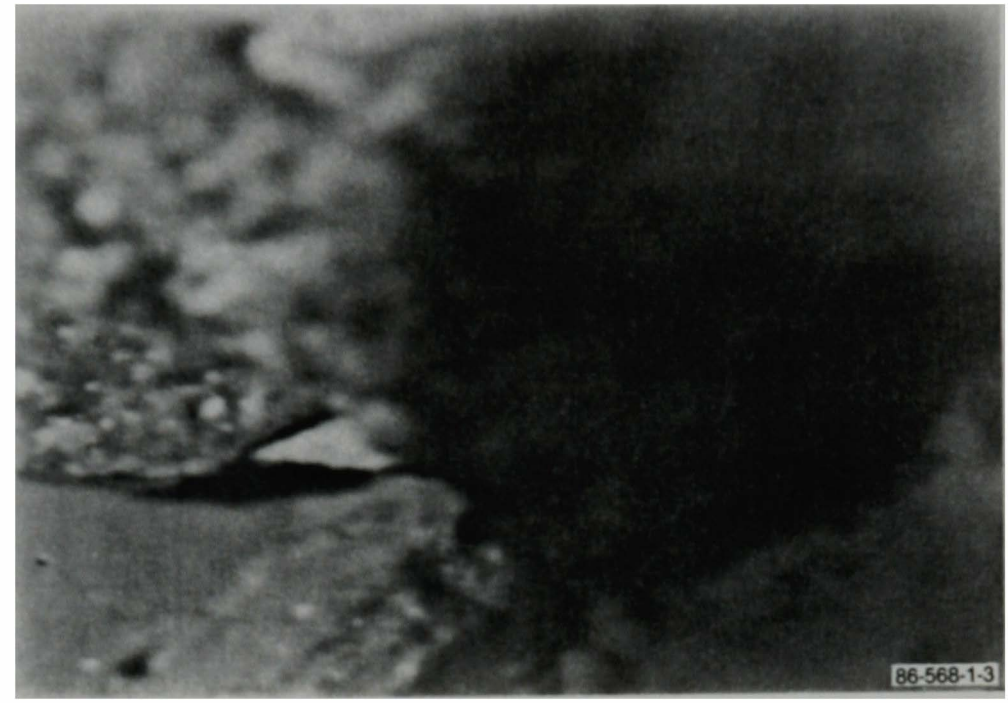

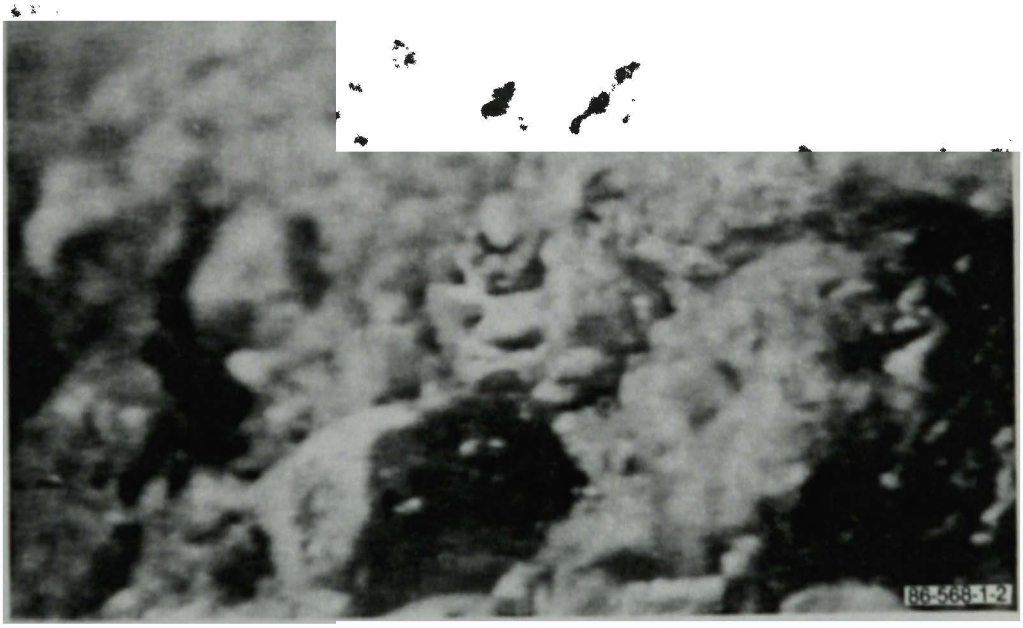

Figure 30. Photographs of large TMI-2 debris chunks at Z axis.

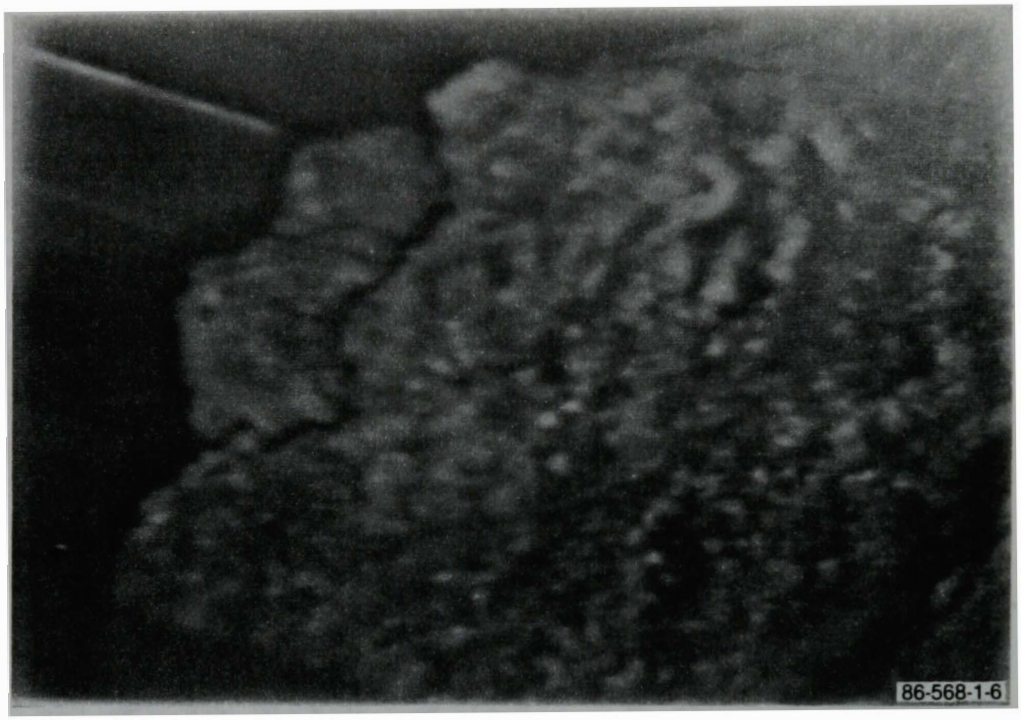

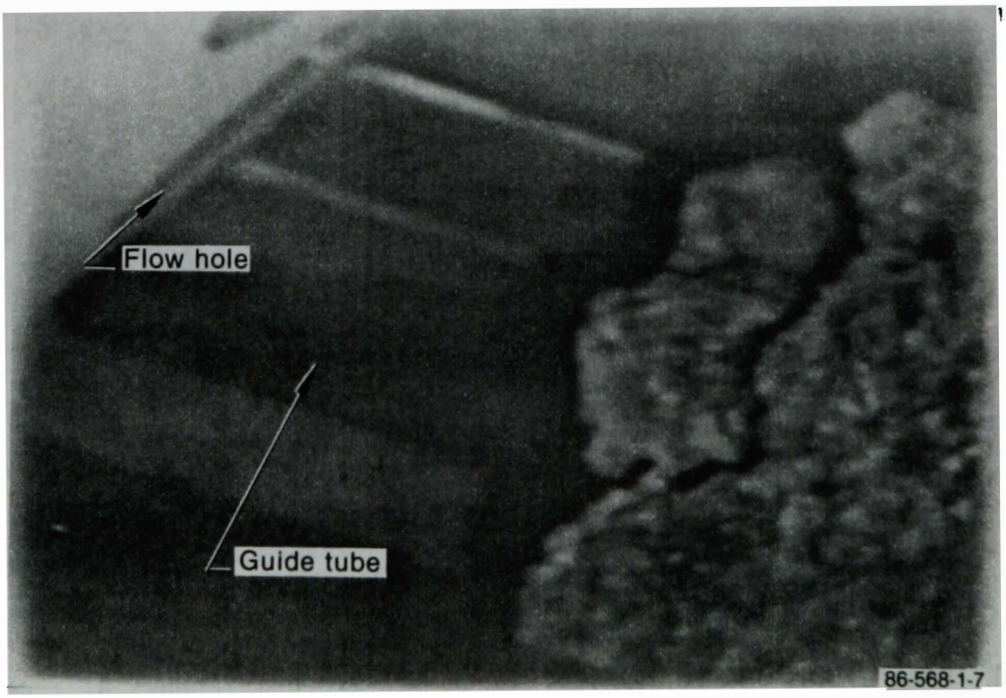

Figure 31. Photographs showing TMI-2 debris chunks in relation to instrumentation guide tube at Z axis.

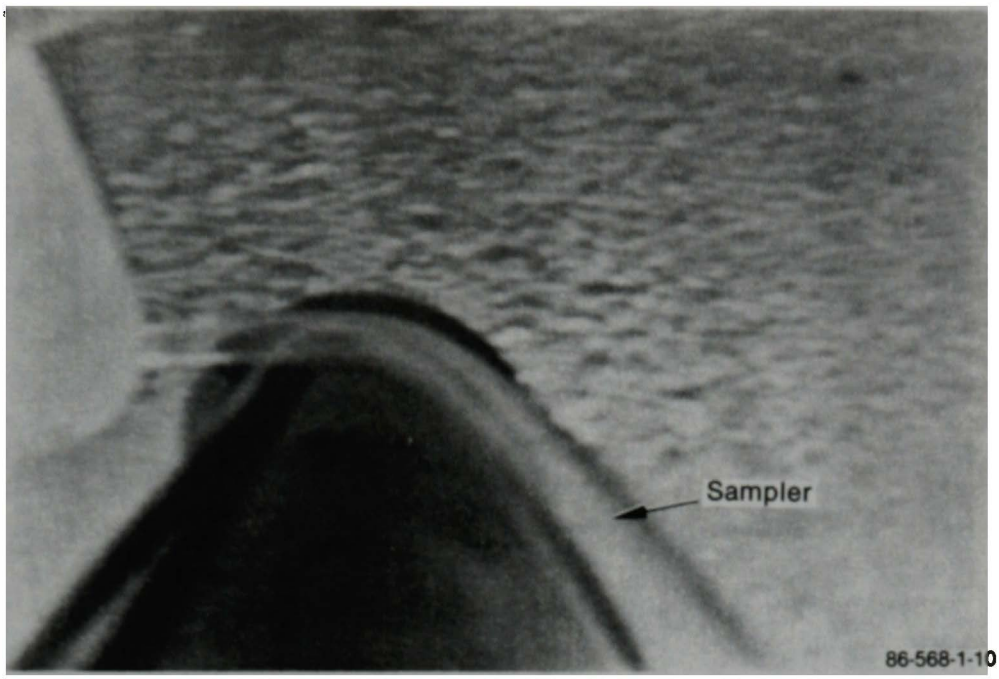

Figure 32. Photograph showing smooth TMI-2 debris surface at W axis.

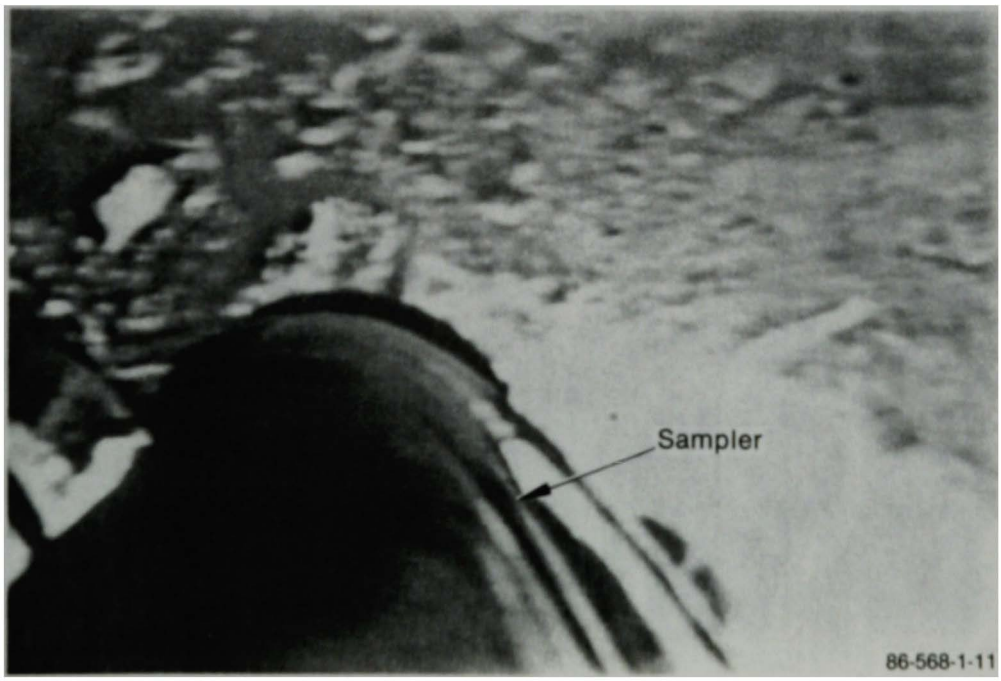

Figure 33. Photograph showing coarse TMI-2 debris on top of smooth surface at W axis.

Figure 34. Photograph of TMI-2 lower plenum debris bed at the K-9 location.

the K-9 location and includes cladding shards which most probably relocated there during the operation. An estimate of the relative sizes of the rubble can be made by comparison with the shard which lies atop the bed (diameter approximately 2.5 cm). As was the case at the W axis, the rubble appears to be very loose and is easily dislodged by the camera.

CONCLUSIONS AND RECOMMENDATIONS

In summary, video data were taken during the lower plenum examinations in February, July, and December 1985 and during the core bore operations in July 1986. These data have been examined, and an estimated contour map of the lower plenum rubble bed has been generated. The rubble bed is fairly flat and ranges from a uniform and smooth bed to a bed with many large chunks interspersed with finer debris. The bed extends to the downcomer wall everywhere except near the Y axis, where a "cliff" of previously molten corium extends to the outer row of instrument guide tubes and then abruptly stops.

Samples have been taken from the lower plenum debris bed during inspection of the W and X axes. It is recommended that additional samples be obtained and analyzed from the Y and Z axes as well to more completely characterize the lower plenum debris bed. This is important so that it can be determined to what extent the debris bed fission product concentration is homogeneous.

REFERENCES

1. V. R. Fricke, Reactor Lower Head Video Inspection, TMI-2 Technical Planning Bulletin 85-6, Rev. 0, February 26, 1985.

2. V. R. Fricke, Reactor Lower Head Video Inspection, TMI-2 Technical Planning Bulletin 85-6, Rev. 1, March 7, 1985.

3. S. Bakharre, Reactor Lower Head Video Inspection, TMI-2 Technical Planning Bulletin 85-23, Rev. 0, August 8, 1985.

4. Letter, J. M. Broughton to W. R. Young, "Data Transmittal, Lower Vessel Debris," JMB-46-86, March 31, 1986.

5. V. R. Fricke, Hydraulic Disturbance of the Debris in the Bottom Head of the TMI-2 Reactor Vessel, TMI-2 Technical Planning Bulletin 85-20, July 26, 1985.

6. D. E. Owen, Reactor Vessel Lower Head Video Inspection - Phase 2, TMI-2 Technical Planning Bulletin 86-03, Rev. 0, January 8, 1986.

7. E. L. Tolman et al., TMI-2 Core Bore Acquisition Summary Report, EGG-TMI-7385, September 1986.

8. S. Bakharre, Crust Breaking via Core Drilling, TMI-2 Technical Planning Bulletin 86-45, Rev. 0, December 4, 1986.

9. R. Rainish, Impacts of Core Drilling Operations on Reactor Vessel Lower Head Rubble Inventory, TMI-2 Technical Planning Bulletin 87-6, Rev. 0, March 30, 1987.

10. G. Worku, Reactor Vessel Lower Head Video Inspection - Phase II, TMI-2 Technical Planning Bulletin 86-03, Rev. 1, March 11, 1987.

11. E. L. Tolman et al., TMI-2 Accident Scenario Update, EGG-TMI-7489, December 1986.

12. C. S. Olsen, D. W. Akers, and R. K. McCardell, Examination of Debris from the Lower Reactor Head of the TMI-2 Reactor (Draft), EGG-TMI-7573, April 1987.

13. J. A. Moore, "A Fuel Rod Debris Packing Model," Nuclear Technology 67, October 1984, pp. 66-72.

14. E. H. Karb et al, KfK In-Pile Tests on LWR Fuel Rod Behavior During the Heatup Phase of a LOCA, KfK-3028, October 1980.

APPENDIX A

TMI-2 LOWER PLENUM INSTRUMENTATION GUIDE TUBE GEOMETRY

APPENDIX A

TMI-2 LOWER PLENUM INSTRUMENTATION GUIDE TUBE GEOMETRY

This Appendix summarizes the geometry of the instrumentation guide tubes in the TMI-2 lower plenum. In order to provide a quantitative interpretation of the lower plenum video data, a series of fiducials was required. Since the various instrumentation guide tubes were, in many cases, visually accessible using the video cameras, the local depth of the debris bed could be measured using the relative depth of the debris bed compared with the instrumentation guide tubes as a reference. The geometry of the guide tubes was researched in order to provide the needed information, and figures A-1 through A-15 show the geometry of each of the guide tubes used in determination of the lower plenum debris bed depth profile. The figures are not drawn to scale; the dimensions on the figures were provided by Owen and Rainish.[a]

The geometries of the guide tubes are azimuthally symmetric. Therefore, guide tubes which are located at the same radius from the core centerline will have the same dimensions. The exception to this is that some guide tubes do not have gussets, whereas others at the same radius do. Table A-1 lists all the guide tubes used in determining the lower plenum debris bed topography and indicates which ones have gussets.

---

a. Private communication, D. E. Owen, January 9, 1986; private communication, R. Rainish, May 29, 1987.

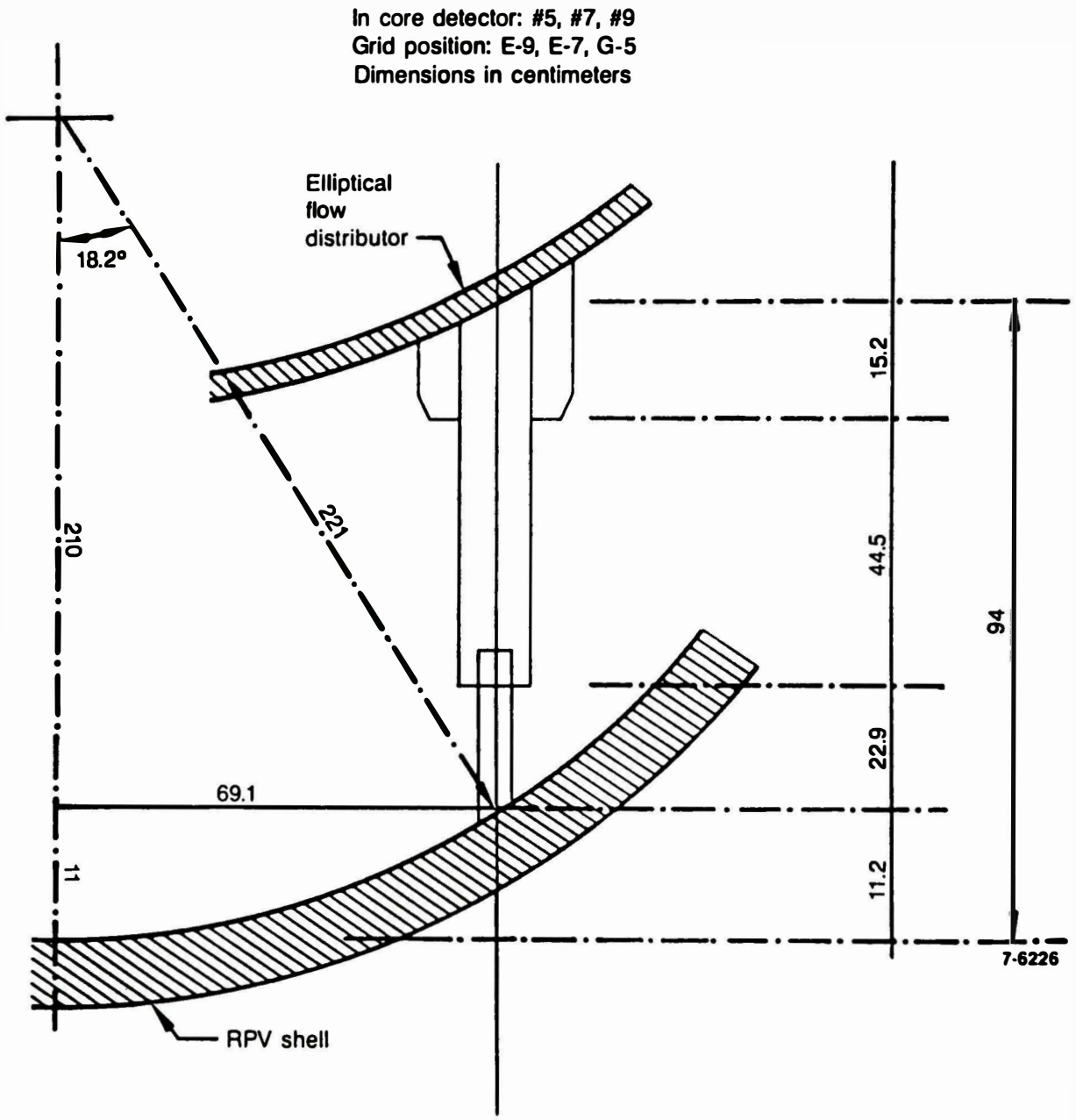

Figure A-1. TMI-2 In-core detector No. 5, 7, or 9 in grid position E-9, F-7, or G-5.

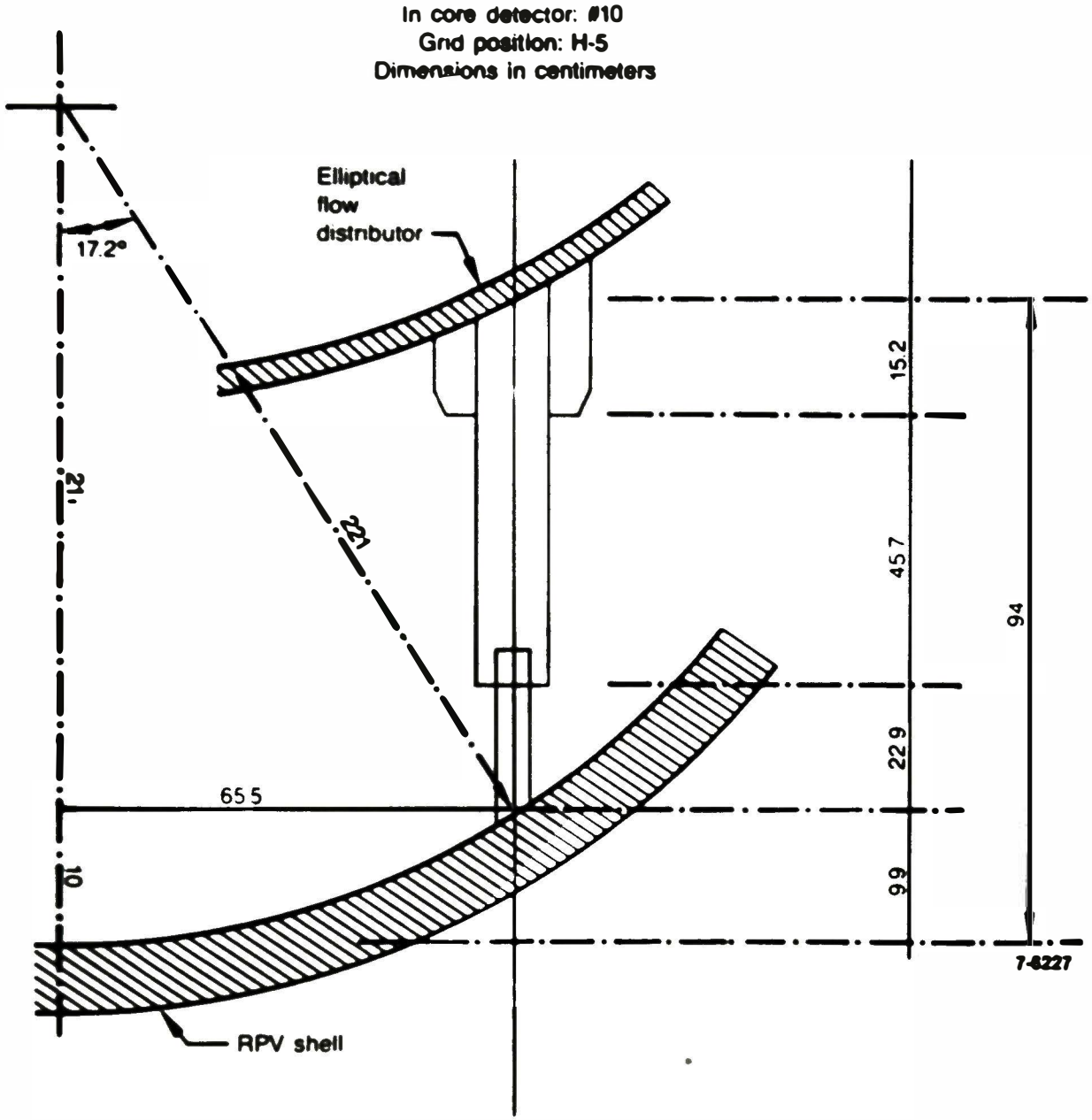

Figure A-2. TMI-2 in-core detector No. 10 in grid position H-5.

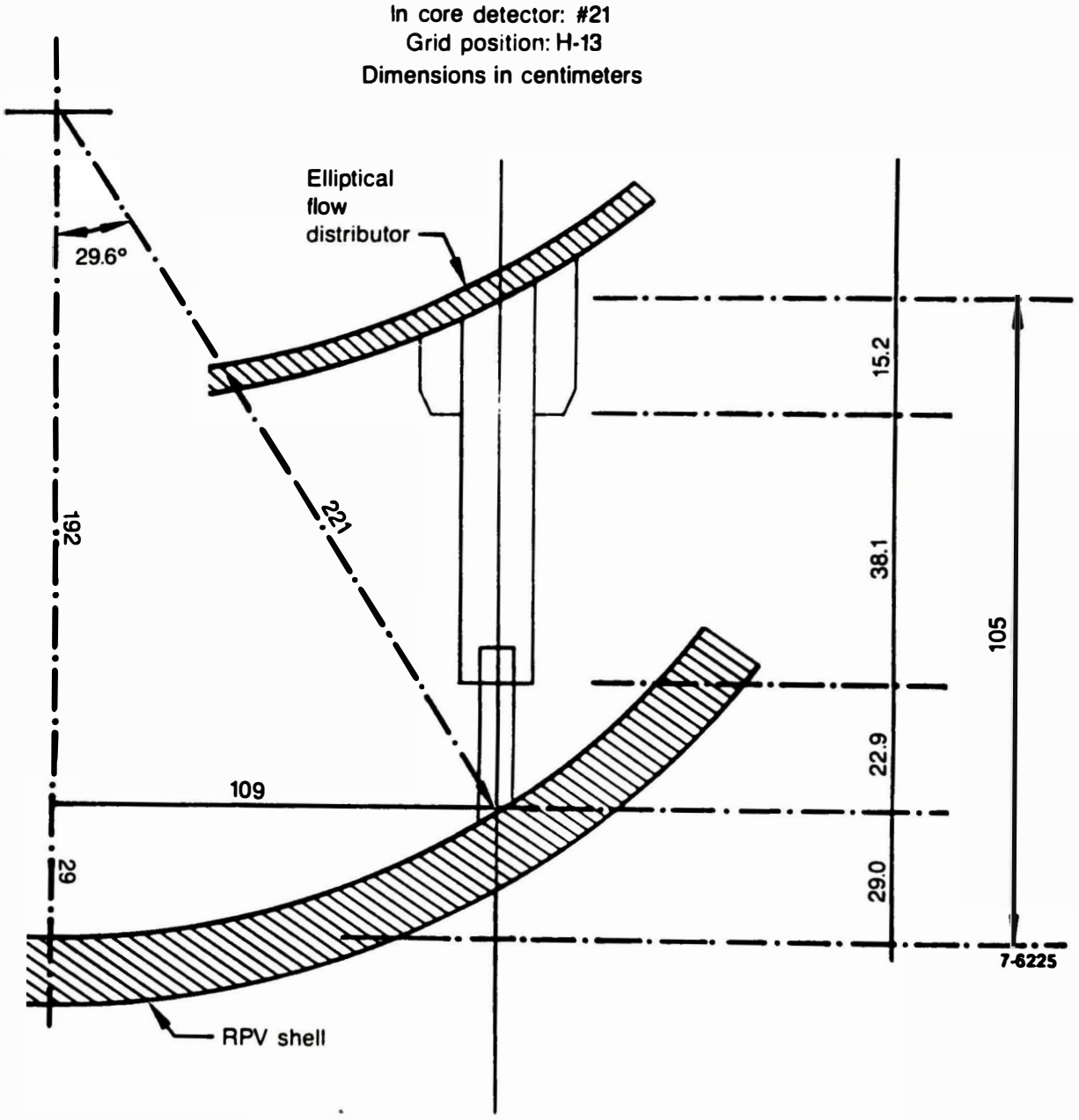

Figure A-3. TMI-2 in-core detector No. 21 in grid position H-13.

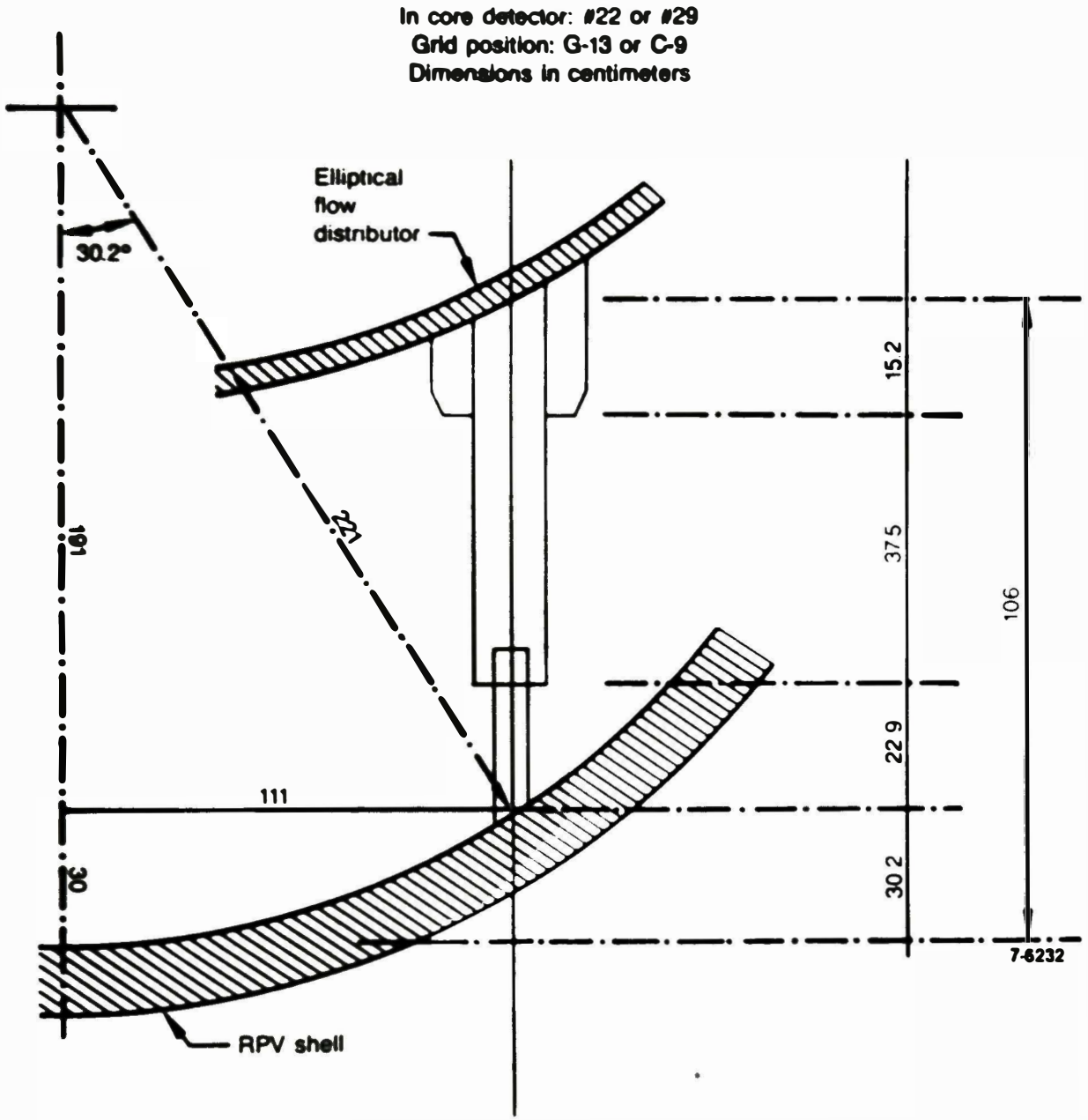

Figure A-4. TMI-2 in-core detector No. 22 or 29 in grid position G-13 or C-9.

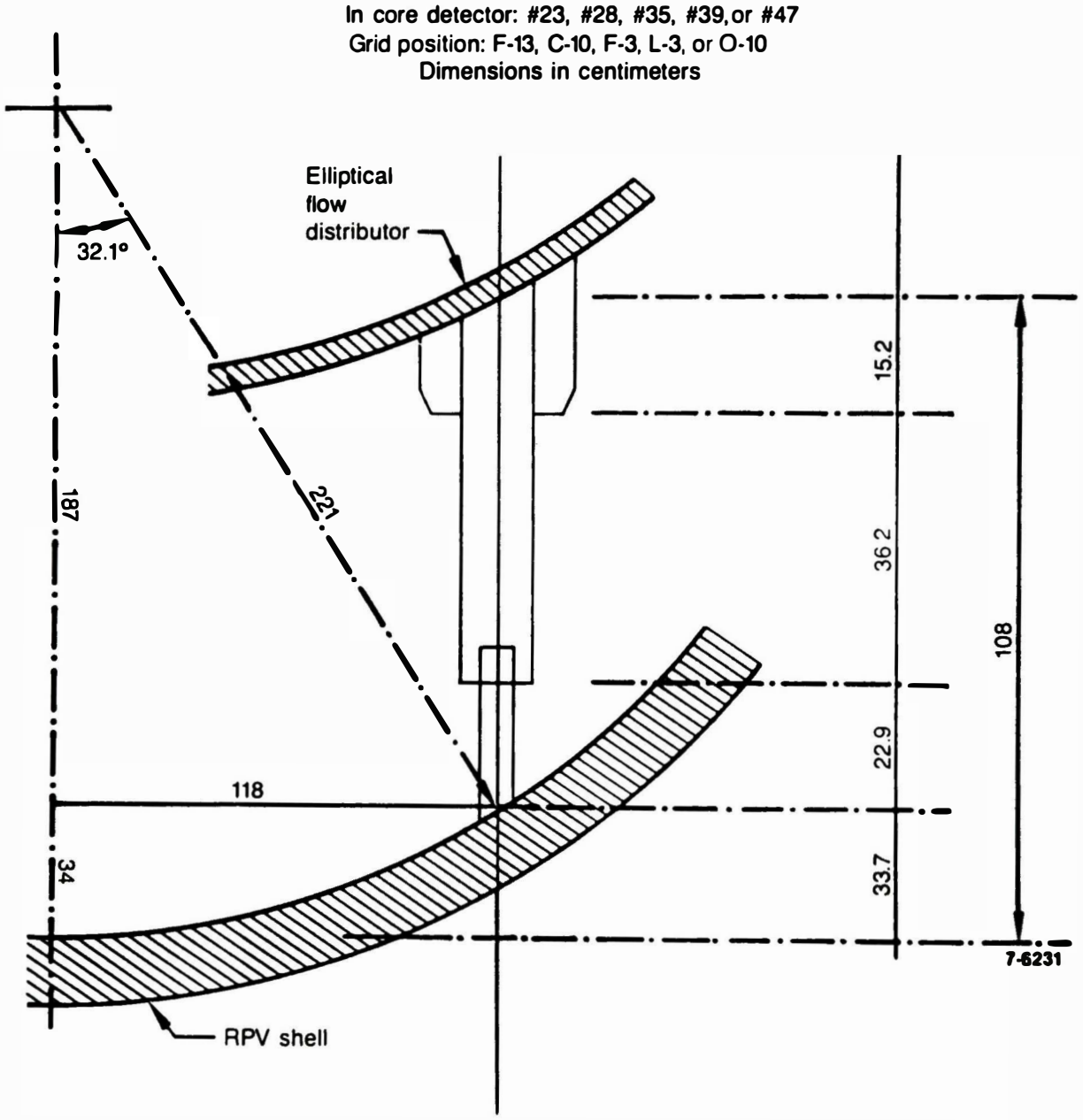

Figure A-5. TMI-2 in-core detector No. 23, 28, 35, 39, or 47 in grid position F-13, C-10, F-3, L-3, or O-10.

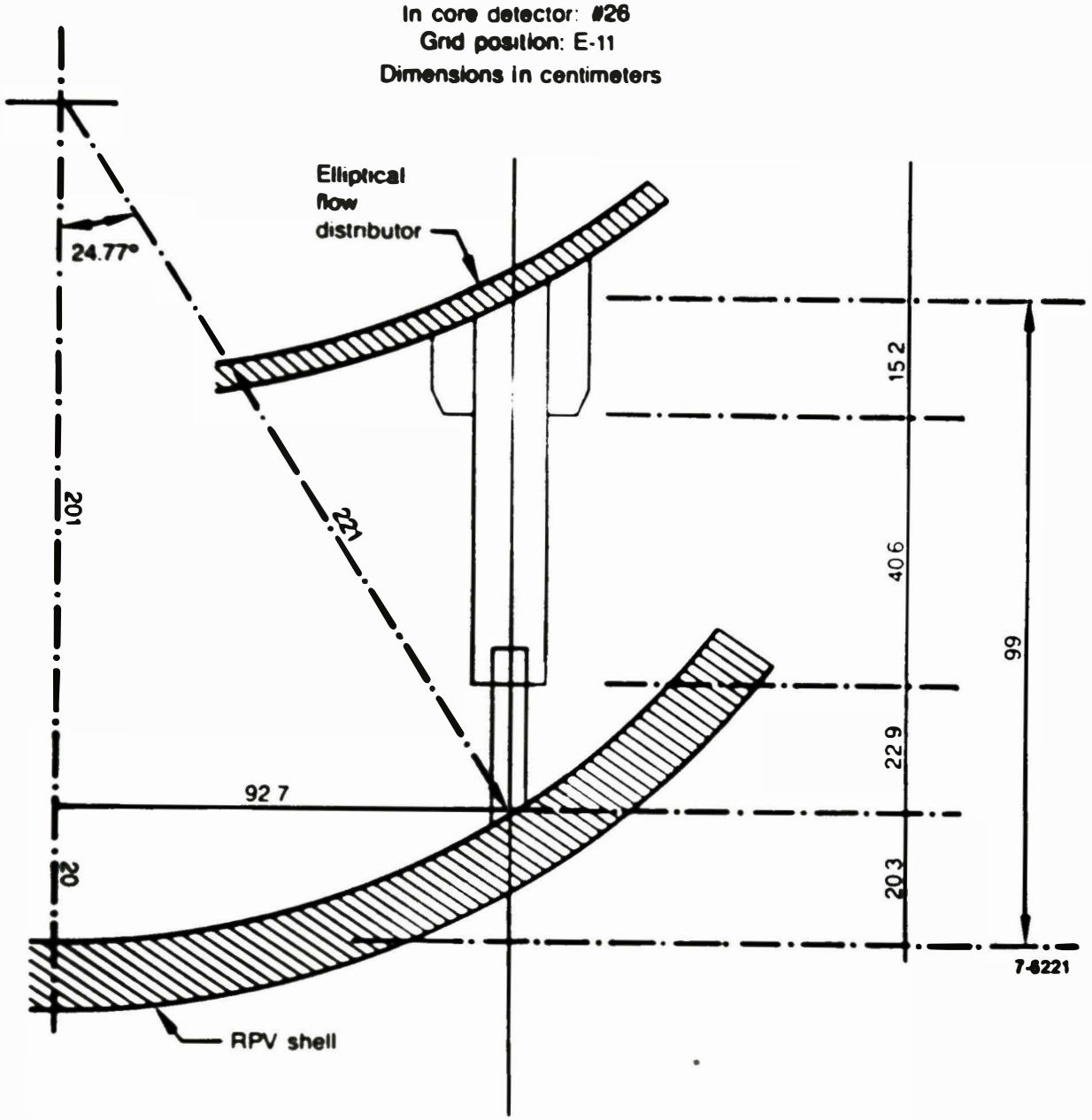

Figure A-6. TMI-2 in-core detector No. 26 in grid position E-11.

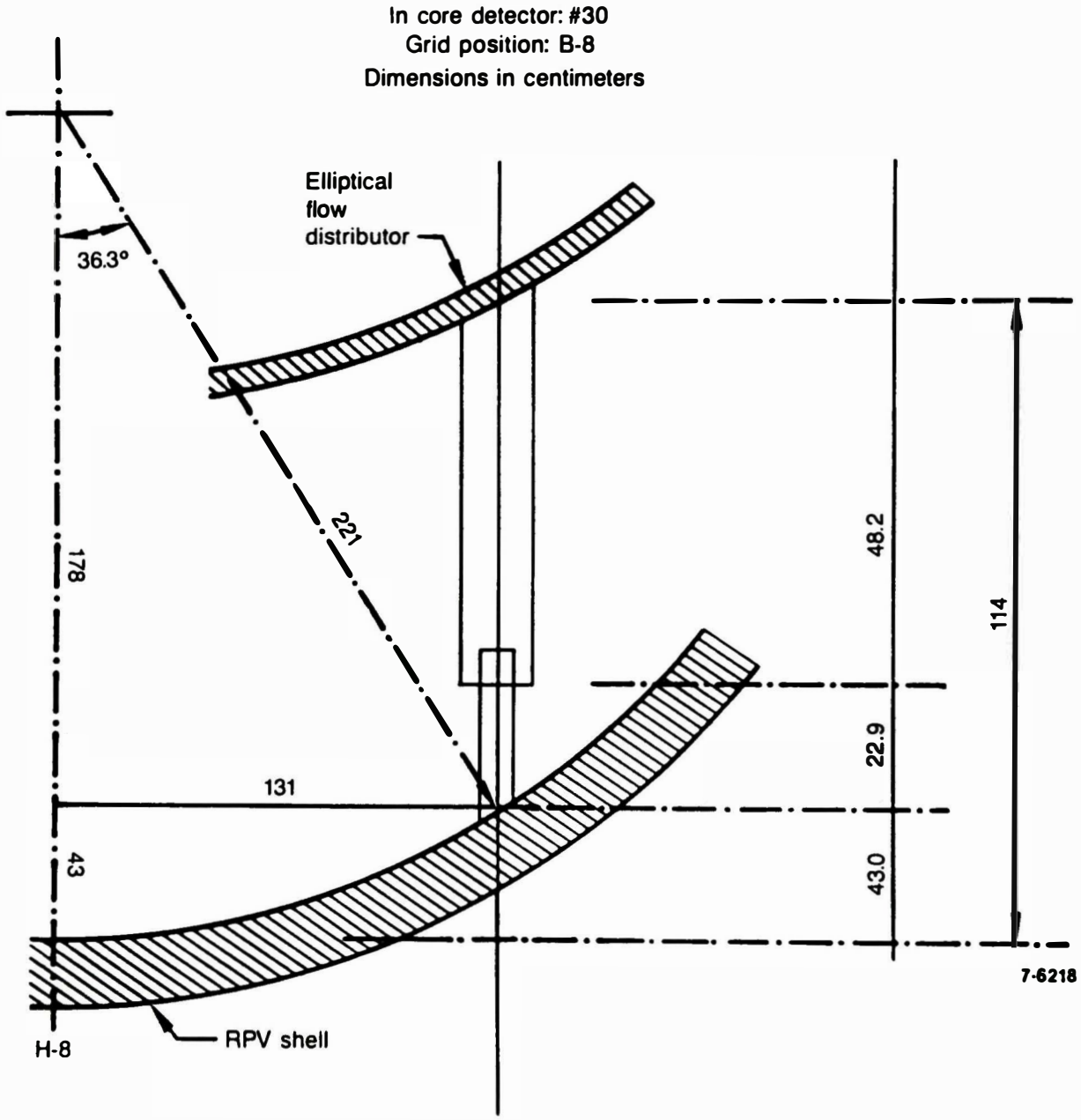

Figure A-7. TMI-2 in-core detector No. 30 in grid position B-8.

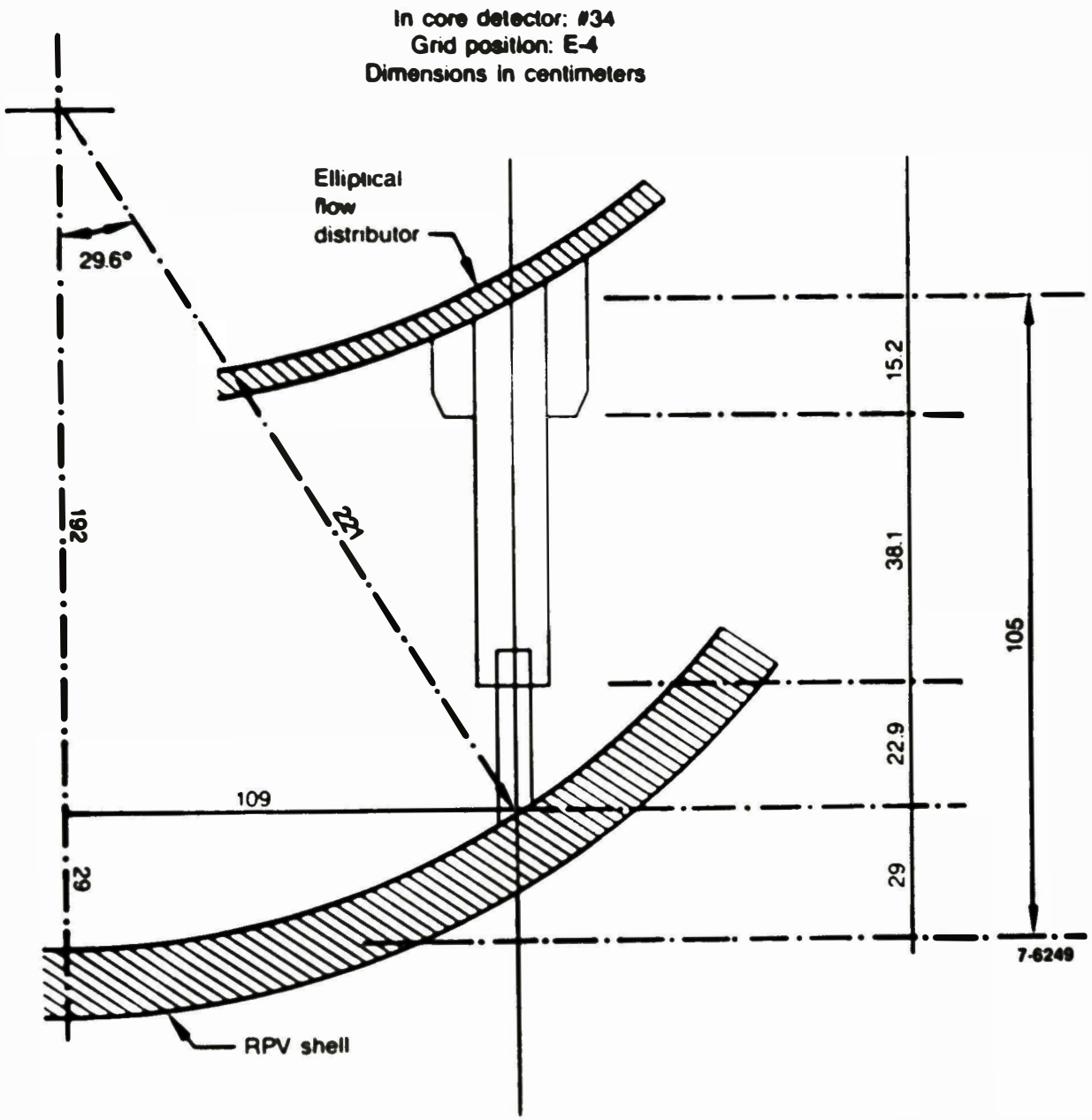

Figure A-8. TMI-2 in-core detector No. 34 in grid position E 4.

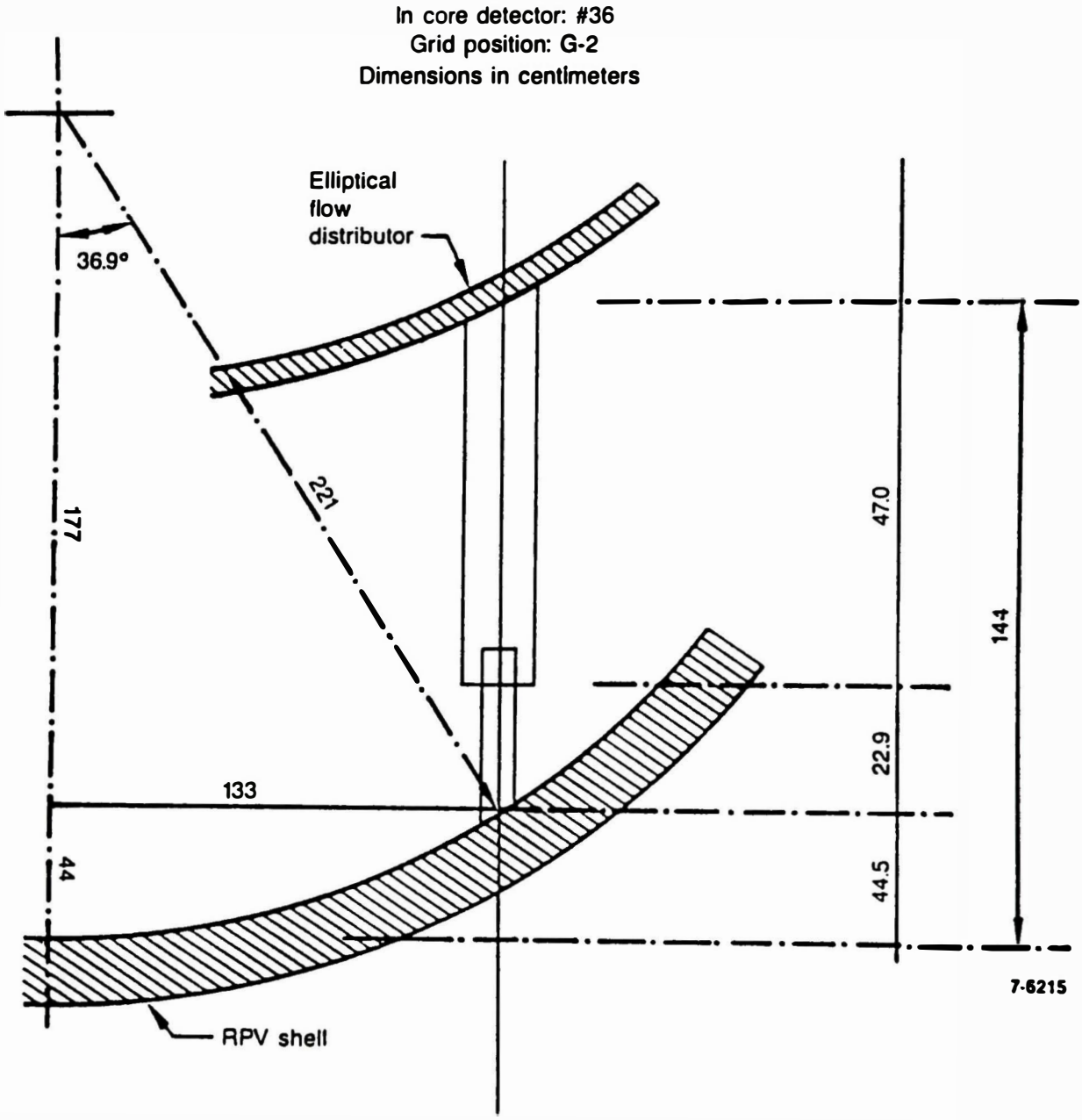

Figure A-9. TMI-2 in-core detector No. 36 in grid position G-2.

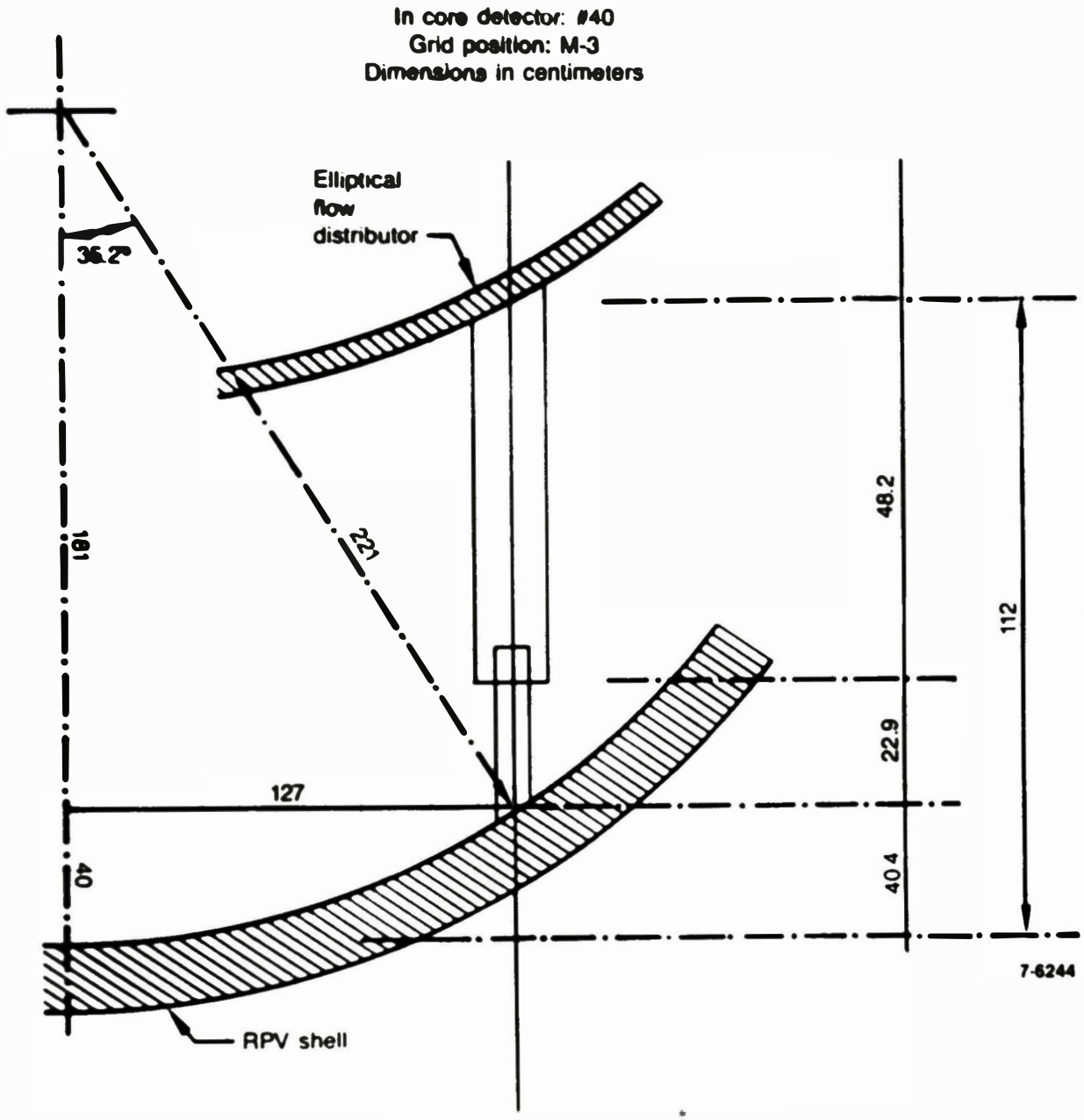

Figure A-10. TMI-2 in-core detector No. 40 in grid position M-3.

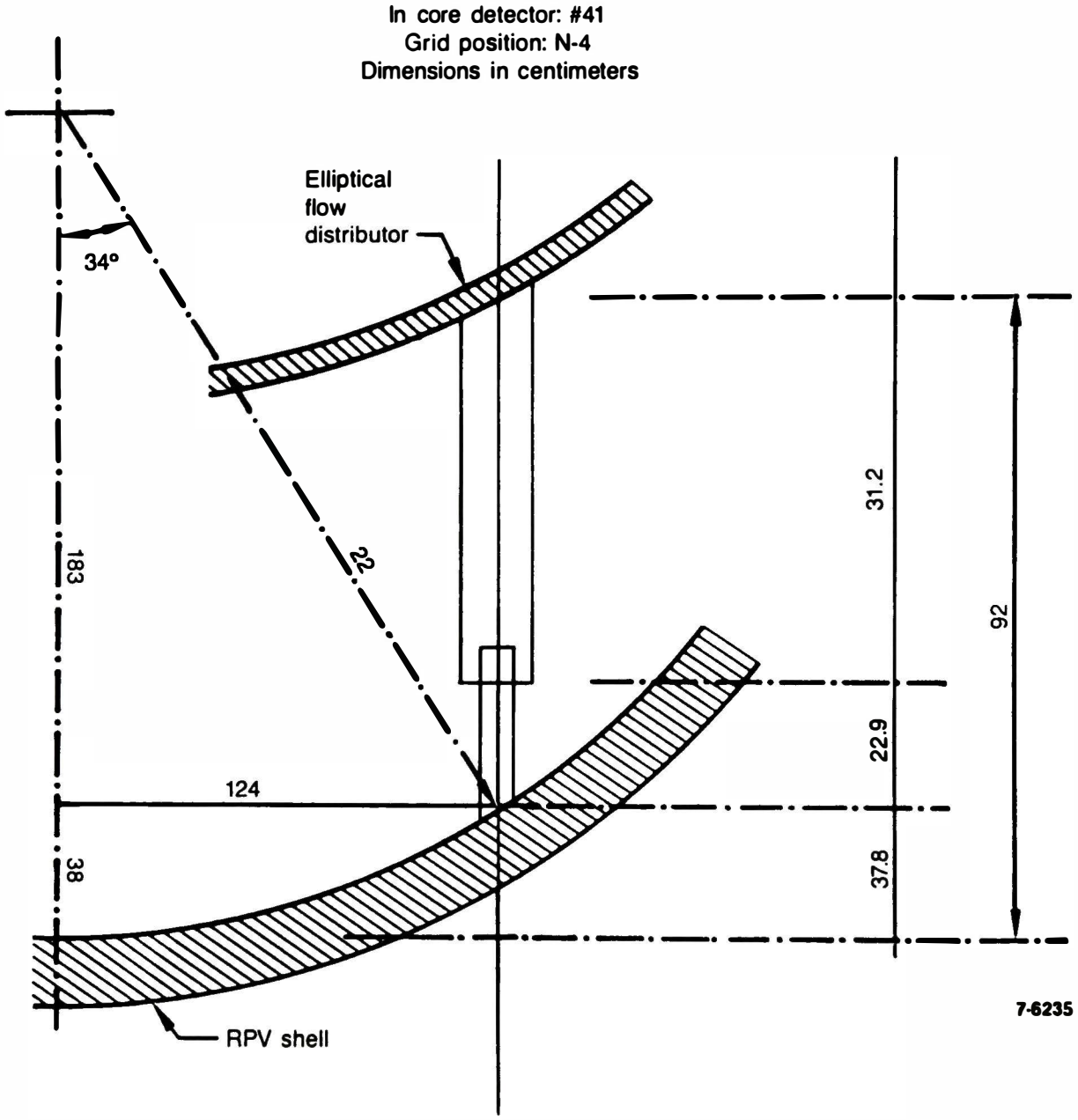

Figure A-11. TMI-2 in-core detector No. 41 in grid position N-4.

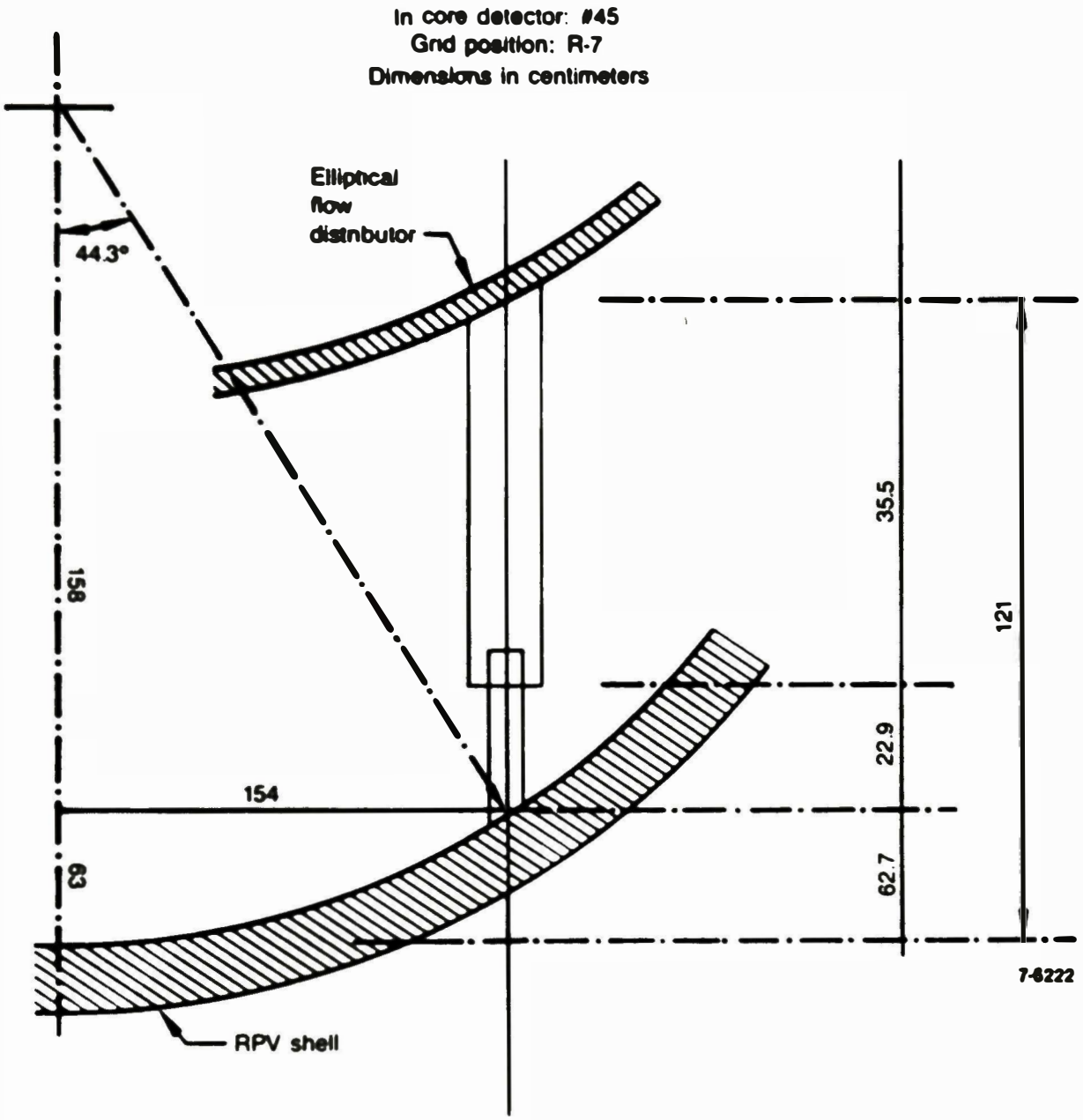

Figure A-12. TMI-2 In-core detector No. 45 in grid position R-7.

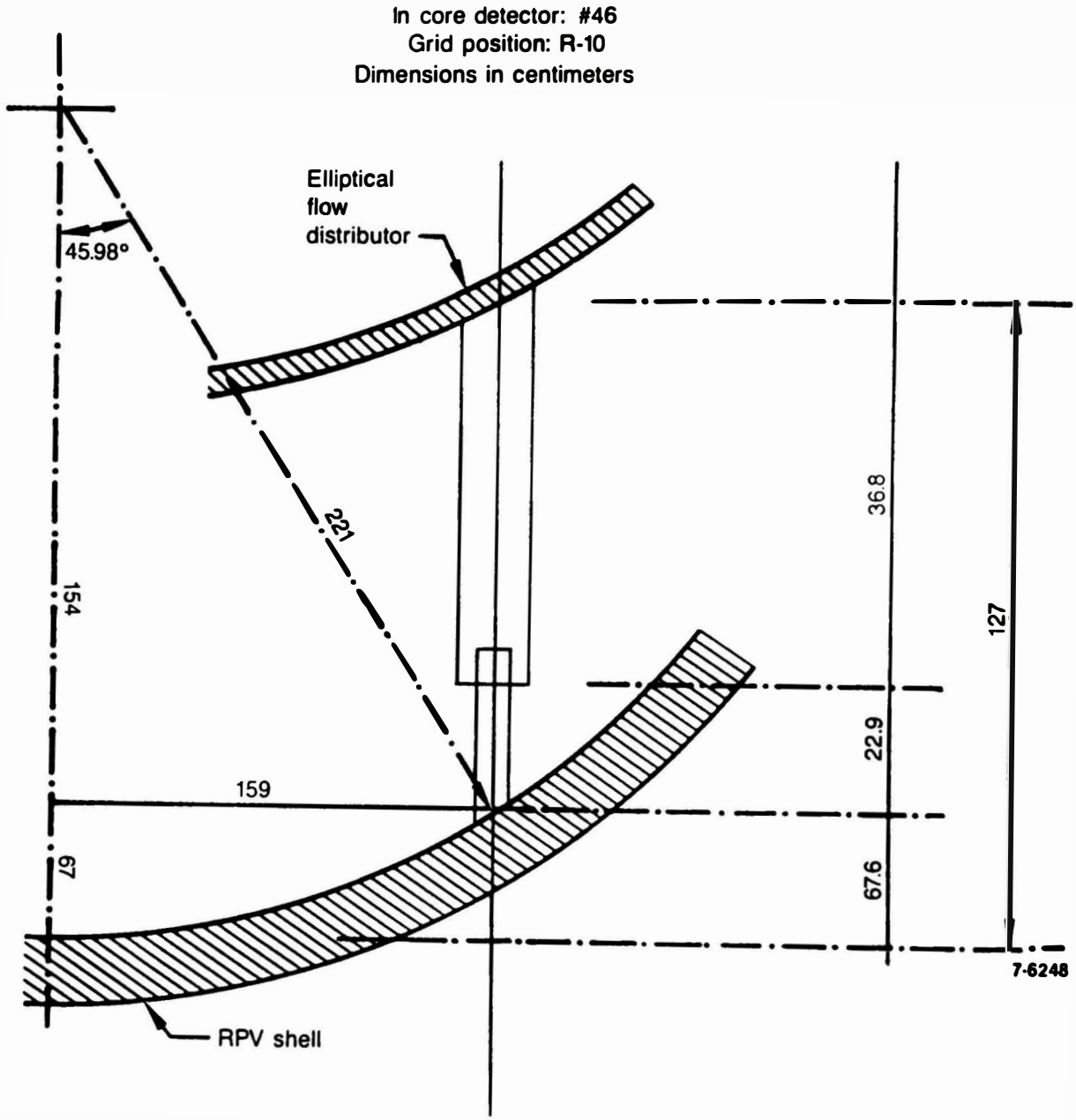

Figure A-13. TMI-2 in-core detector No. 46 in grid position R-10.

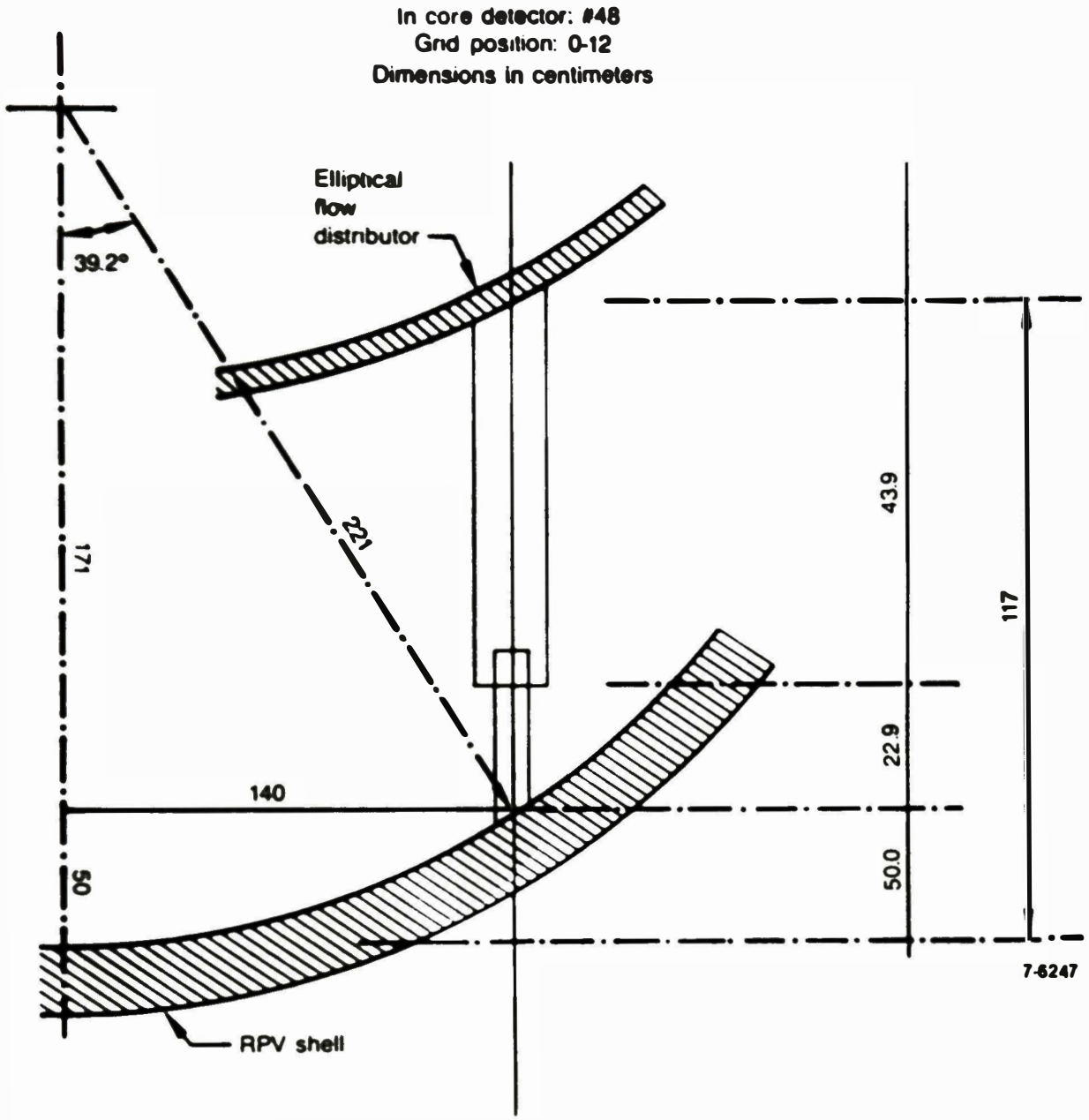

Figure A-14. TMI-2 in-core detector No. 48 in grid position 0-12.

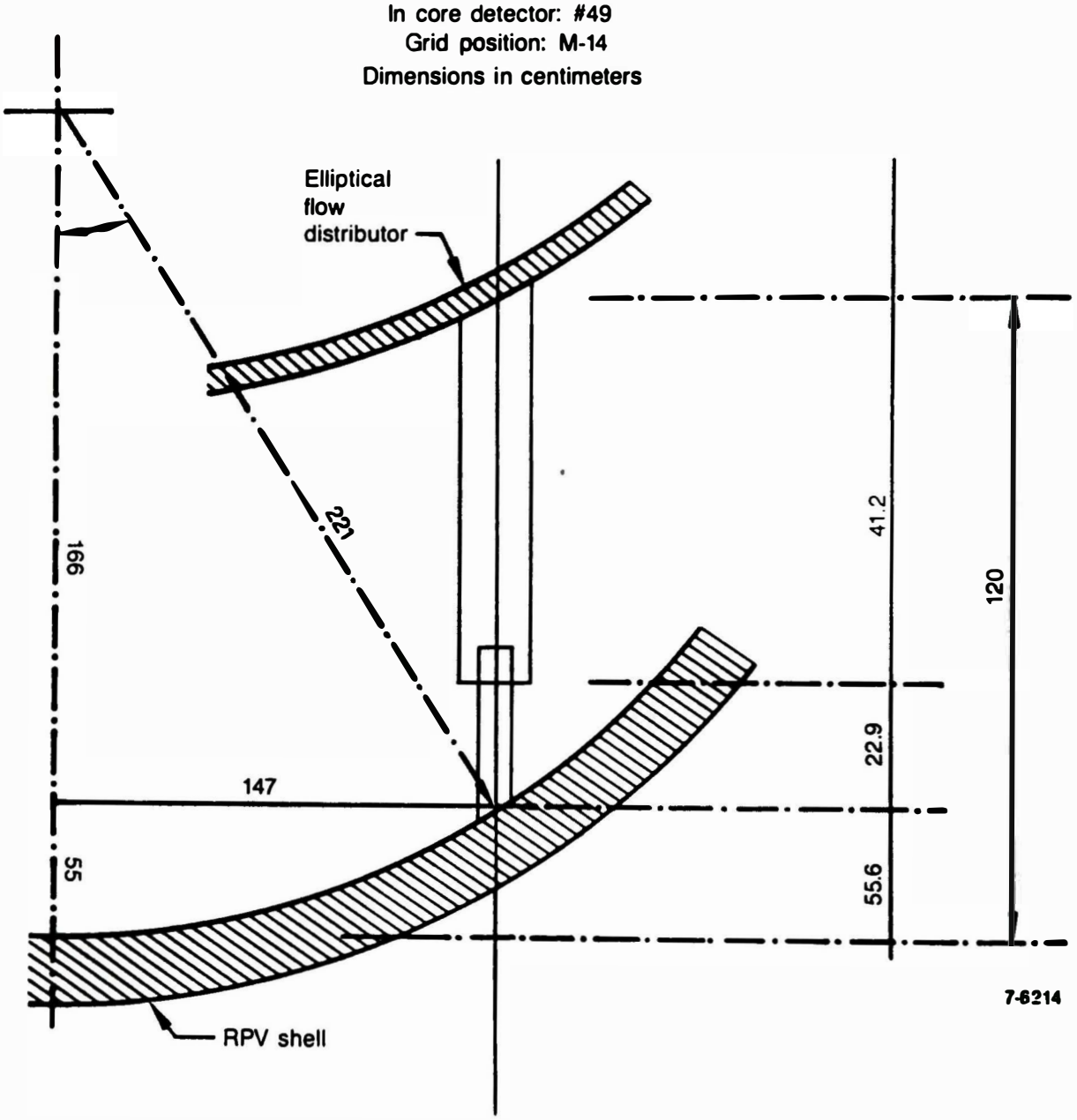

Figure A-15. TMI-2 in-core detector No. 49 in grid position M-14.

TABLE A-1. GUIDE TUBES USED IN LOWER PLENUM DEBRIS BED VOLUME DETERMINATION

Guide Tube	Grid Location	Gusset	Figure
5	E-9	Yes	A-1
7	E-7	Yes	A-1
9	G-5	Yes	A-1
10	H-5	Yes	A-2
21	H-13	Yes	A-3
22	G-13	Yes	A-4
23	F-13	Yes	A-5
26	E-11	Yes	A-6
28	C-10	Yes	A-5
29	C-9	Yes	A-4
30	B-8	No	A-7
34	E-4	Yes	A-8
35	F-3	Yes	A-5
36	G-2	No	A-9
39	L-3	Yes	A-5
40	M-4	No	A-10
41	N-4	No	A-11
45	R-7	No	A-12
46	R-10	No	A-13
47	O-10	Yes	A-4
48	O-12	No	A-14
49	M-14	No	A-15

APPENDIX B

RESULTS FROM FEBRUARY 1987 VIDEO INSPECTION

APPENDIX B

RESULTS FROM FEBRUARY 1987 VIDEO INSPECTION

An inspection of the southeast quadrant of the lower plenum was made on February 21, 1987. This inspection was made by lowering the video camera down inspection hole No. 5 in the downcomer. The camera was attached to a suction device that was used to remove the fine debris from around guide tube 45 at grid location R-7 for better viewing. Much of the debris in this area had located there as a result of the extensive boring operation of the hard crust in the core region. (Several hundred holes were bored in the crust in an attempt to break up the crust for removal.) Thus, the debris bed had been perturbed and it no longer is representative of that which existed just after the accident. Because of this, no additional debris bed depth or composition information is available from this inspection.

The condition of guide tube 45 was clearly visible during the inspection. This guide tube experienced thermal attack during the relocation of the core into the lower plenum. The results of this thermal attack are evident on Figure B-1, which is a series of enhanced photographs taken from the video data. The edge of the guide tube is severely ablated, and the instrument penetration tube may also have experienced thermal attack, though it is difficult to see the latter in these photographs.

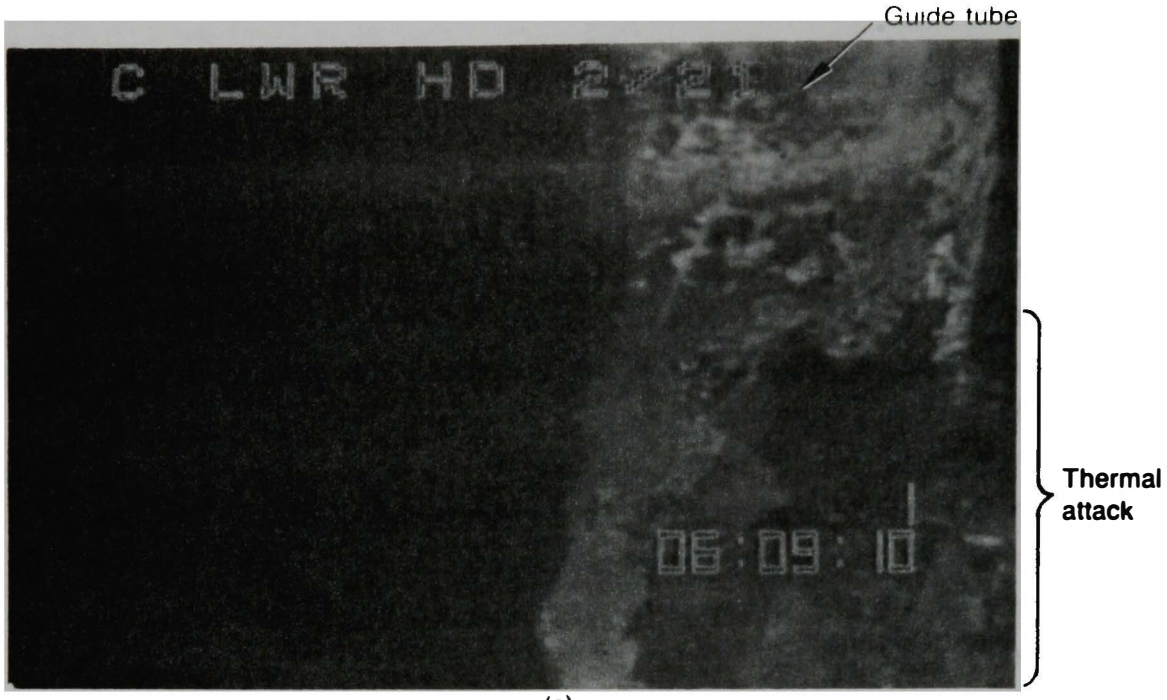

Figure B-1. Enhanced photograph of guide tube #45, core position R-7.

(e)

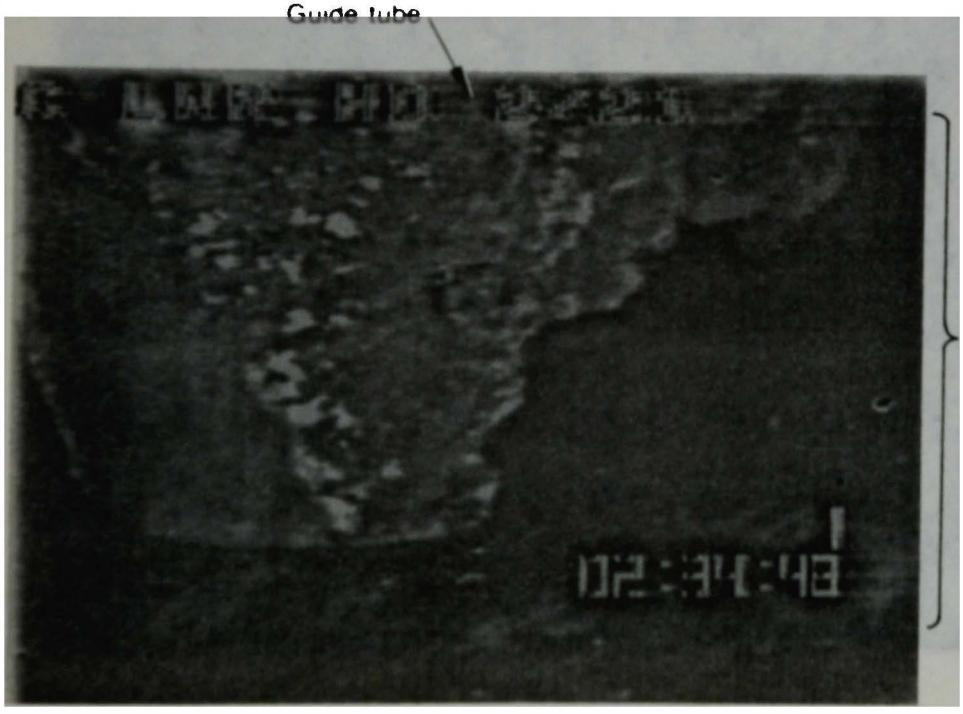

(f)

Figure B-1. (continued)

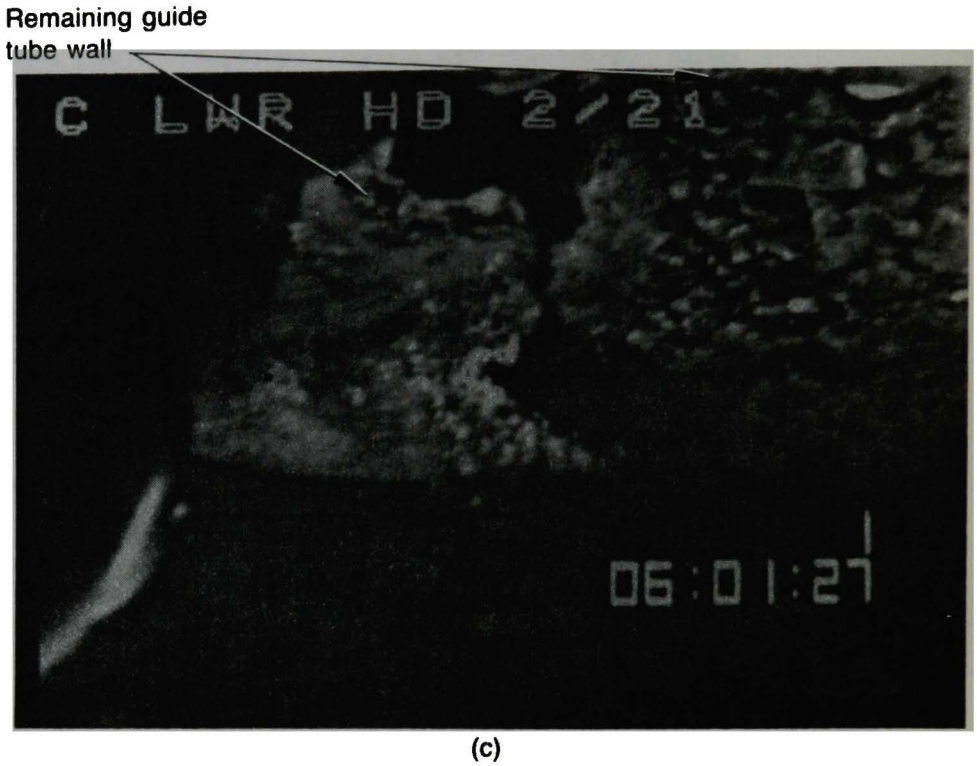

(c)

(d)

Figure B-1. (continued)